AD-A140 221 FATIGUE CONSIDERATIONS IN VIEW OF MEASURED LOAD SPECTRA 1/1
(U) TELEDYNE ENGINEERING SERVICES WALTHAM MA
W G DOBSON ET AL. 1983 TR-3049-4 SSC-315 DOT-CG-80359-A
UNCLASSIFIED F/G 20/11 NL

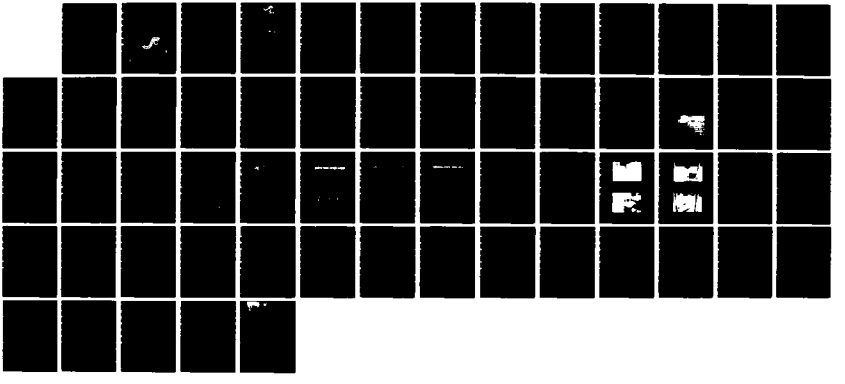

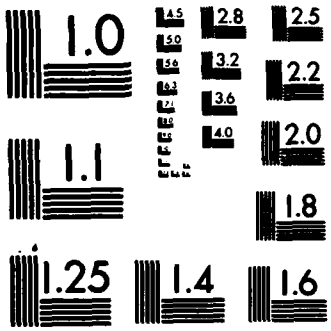

SSC-315

FATIGUE CONSIDERATIONS IN VIEW OF MEASURED LOAD SPECTRA

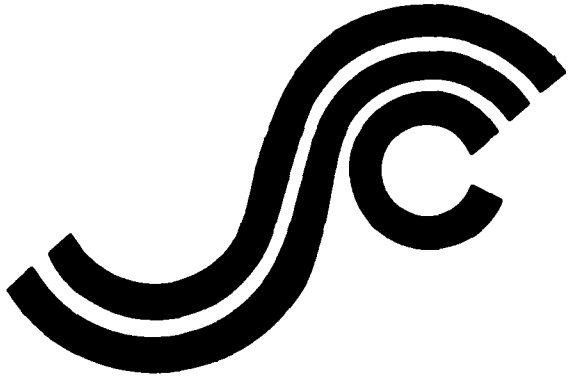

SHIP STRUCTURE COMMITTEE

1983

SHIP STRUCTURE COMMITTEE

The SHIP STRUCTURE COMMITTEE is constituted to prosecute a research program to improve the hull structures of ships and other marine structures by an extension of knowledge pertaining to design, materials and methods of construction.

RAdm Clyde T. Lusk, Jr., USCG (Chairman)
Chief, Office of Merchant Marine Safety
U. S. Coast Guard Headquarters

Mr. J. Gross
Deputy Assistant Administrator for Commercial Development
Maritime Administration

Mr. P. M. Palermo
Executive Director
Ship Design & Integration Directorate
Naval Sea Systems Command

Mr. J. B. Gregory
Chief, Research & Development Staff of Planning & Assessment
U.S. Geological Survey

Mr. W. N. Hannan
Vice President
American Bureau of Shipping

Mr. Thomas W. Allen
Chief Engineering Officer
Military Sealift Command

LCdr D. B. Anderson, U.S. Coast Guard (Secretary)

SHIP STRUCTURE SUBCOMMITTEE

The SHIP STRUCTURE SUBCOMMITTEE acts for the Ship Structure Committee on technical matters by providing technical coordination for the determination of goals and objectives of the program, and by evaluating and interpreting the results in terms of structural design, construction and operation.

U. S. COAST GUARD

CAPT A.E. HENN
MR. J.S. SPENCER
MR. R.E. WILLIAMS
LCDR K.G. ZIMMERMAN

NAVAL SEA SYSTEMS COMMAND

MR. J. B. O'BRIEN (CHAIRMAN)
CDR E. RUNNERSTROM
MR. J.E. GAGORIK
MR. C.T. LOESER
MR. S.G. ARNTSON (COTR)
MR. G. WOODS (COTR)

MARITIME ADMINISTRATION

MR. F. SEIBOLD
MR. N.O. HAMMER
DR. W.M. MACLEAN
MR. M.W. TOUMA

NATIONAL ACADEMY OF SCIENCES
COMMITTEE ON MARINE STRUCTURES

MR. A. DUDLEY HAFF - LIAISON
MR. R.W. RUMKE - LIAISON

SOCIETY OF NAVAL ARCHITECTS & MARINE ENGINEERS

MR. N.O. HAMMER - LIAISON
MR. F. SELLARS - LIAISON

WELDING RESEARCH COUNCIL

DR. G. W. OYLER - LIAISON

MILITARY SEALIFT COMMAND

MR. D. STEIN
MR. T.W. CHAPMAN
MR. A. ATTERMEYER
MR. A.B. STAVOVY

AMERICAN BUREAU OF SHIPPING

DR. D. LIU
MR. I. L. STERN

MINERALS MANAGEMENT SERVICE

MR. R. GIANGERELLI
MR. C.E. SMITH

INTERNATIONAL SHIP STRUCTURES CONGRESS

MR. S.G. STIANSEN - LIAISON

AMERICAN IRON & STEEL INSTITUTE

MR. J. J. SCHMIDT - LIAISON

STATE UNIVERSITY OF NY MARITIME COLLEGE

DR. W.R. PORTER - LIAISON

U.S. COAST GUARD ACADEMY

LT J. TUTTLE - LIAISON

U.S. NAVAL ACADEMY

DR. R. BHATTACHARYYA - LIAISON

U.S. MERCHANT MARINE ACADEMY

DR. C.M. KIM - LIAISON

Member Agencies:

United States Coast Guard
Naval Sea Systems Command
Military Sealift Command
Maritime Administration
United States Geological Survey
American Bureau of Shipping

Ship Structure Committee

An Interagency Advisory Committee
Dedicated to Improving the Structure of Ships

Address Correspondence to:

Secretary, Ship Structure Committee
U.S. Coast Guard Headquarters,(G-M/TP 13)
Washington, D.C. 20593

13 JAN 1984

SR-1254

This report documents experimental work, including data analysis, used in assessing the characteristics of fatigue crack propagation under load spectra typical of those experienced by ships at sea. Such information was obtained from the SL-7 containership instrumentation program. Results of these random loadings are compared with constant amplitude loadings.

Clyde T. Lusk, Jr.
Rear Admiral, U.S. Coast Guard
Chairman, Ship Structure Committee

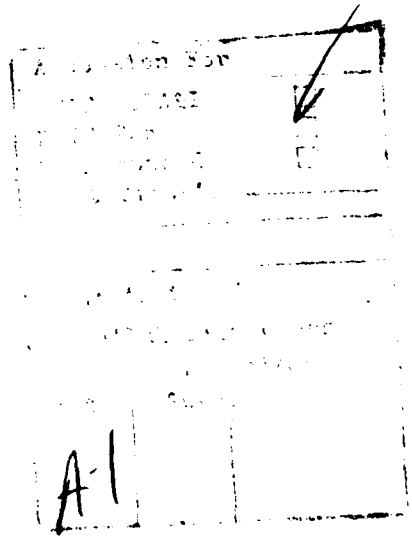

Technical Report Documentation Page

1. Report No.	2. Government Accession No.	3. Recipient's Catalog No.
SSC-315	AD-A140 221	

4. Title and Subtitle	5. Report Date
Fatigue Considerations in View of Measured Load Spectra	1982
	6. Performing Organization Code: SR-1254
7. Author(s) W. G. Dobson, R. F. Brodrick, J. W. Wheaton, J. Giannotti, K. A. Stambaugh	8. Performing Organization Report No.: 3049-4
9. Performing Organization Name and Address: Teledyne Engineering Services, 130 Second Avenue, Waltham, MA 02254	10. Work Unit No. (TRAIS)
	11. Contract or Grant No.: DOT-CG-80359-A
12. Sponsoring Agency Name and Address: U. S. COAST GUARD, 2100 Second Avenue, Washington, D. C. 20593	13. Type of Report and Period Covered: Final
	14. Sponsoring Agency Code

15. Supplementary Notes

SHIP STRUCTURE COMMITTEE FUNDING

16. Abstract

Crack propagation in HY-80 and CS ship steel under typical ship loading time-histories was studied. The loading histories were selected from recorded service stress data which were generated during voyages by the SL-7 containership. Samples of the data were imposed on laboratory specimens as a tape loop signal speeded up by a factor of 25.

Analysis of the results indicated that the crack growth during this random loading compared closely with that of constant-amplitude loading if the stress intensity range were expressed as the root-mean-square. It was also determined that significant crack growth retardation effects were present and that omission of low-amplitude high-frequency components of the loading had little effect on the time rate of growth of cracks.

The potentially large effects of environment on crack growth rate were recognized but were not included in the scope of this work.

17. Key Words	18. Distribution Statement
Fatigue, Fracture Mechanics, Crack Growth, Random Loading	Document is available to the U.S. public through the National Technical Information Service, Springfield, VA 22161

19. Security Classif. (of this report)	20. Security Classif. (of this page)	21. No. of Pages	22. Price
		47 + viii	

Form DOT F 1700.7 (8-72) Reproduction of completed page authorized

METRIC CONVERSION FACTORS

Approximate Conversions to Metric Measures

Symbol	When You Know	Multiply by	To Find	Symbol
	LENGTH			
in	inches	*2.5	centimeters	cm
ft	feet	30	centimeters	cm
yd	yards	0.9	meters	m
mi	miles	1.6	kilometers	km
	AREA			
in^2	square inches	6.5	square centimeters	cm^2
ft^2	square feet	0.09	square meters	m^2
yd^2	square yards	0.8	square meters	m^2
mi^2	square miles	2.6	square kilometers	km^2
	acres	0.4	hectares	ha
	MASS (weight)			
oz	ounces	28	grams	g
lb	pounds	0.45	kilograms	kg
	short tons (2000 lb)	0.9	tonnes	t
	VOLUME			
tsp	teaspoons	5	milliliters	ml
Tbsp	tablespoons	15	milliliters	ml
fl oz	fluid ounces	30	milliliters	ml
c	cups	0.24	liters	l
pt	pints	0.47	liters	l
qt	quarts	0.96	liters	l
gal	gallons	3.8	liters	l
ft^3	cubic feet	0.03	cubic meters	m^3
yd^3	cubic yards	0.76	cubic meters	m^3
	TEMPERATURE (exact)			
°F	Fahrenheit temperature	5/9 (after subtracting 32)	Celsius temperature	°C

*1 in = 2.54 (exactly). For other exact conversions and more detailed tables, see NBS Misc. Publ. 286, Units of Weights and Measures, Price $2.25, SD Catalog No. C13.10:286.

Approximate Conversions from Metric Measures

Symbol	When You Know	Multiply by	To Find	Symbol
	LENGTH			
mm	millimeters	0.04	inches	in
cm	centimeters	0.4	inches	in
m	meters	3.3	feet	ft
m	meters	1.1	yards	yd
km	kilometers	0.6	miles	mi
	AREA			
cm^2	square centimeters	0.16	square inches	in^2
m^2	square meters	1.2	square yards	yd^2
km^2	square kilometers	0.4	square miles	mi^2
ha	hectares (10,000 m^2)	2.5	acres	
	MASS (weight)			
g	grams	0.035	ounces	oz
kg	kilograms	2.2	pounds	lb
t	tonnes (1000 kg)	1.1	short tons	
	VOLUME			
ml	milliliters	0.03	fluid ounces	fl oz
l	liters	2.1	pints	pt
l	liters	1.06	quarts	qt
l	liters	0.26	gallons	gal
m^3	cubic meters	35	cubic feet	ft^3
m^3	cubic meters	1.3	cubic yards	yd^3
	TEMPERATURE (exact)			
°C	Celsius temperature	9/5 (then add 32)	Fahrenheit temperature	°F

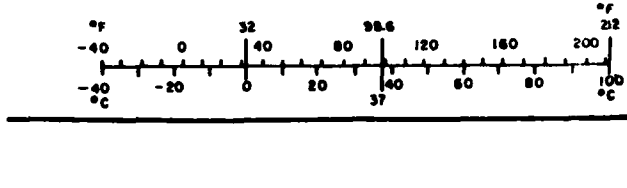

TABLE OF CONTENTS

LIST OF FIGURES

LIST OF FIGURES (Continued)

LIST OF TABLES

1.0 INTRODUCTION

1.1 General

This final report covers the experimental work and data analysis performed by Teledyne Engineering Services (TES) in assessing the characteristics of fatigue crack propagation under load spectra typical of those experienced by ships at sea.

Important inputs to the study were made by Gianotti and Associates (G&A) in developing methodology for defining fatigue load spectra, combined long-term statistical distribution of ship stresses and for determining the proper characteristics of recorded ship stress data for use in the experimental program.

1.2 Background

The procedures used in the design of ships and marine structures have undergone a continuing evolution throughout history. This evolutionary process has not ceased and, in fact, may be in an accelerating phase which has resulted from recently improved knowledge in the fields of fracture mechanics and of fatigue under random loading.

These two fields of knowledge are particularly relevant to the design of ships and marine structures since: a) the initial (and most advanced) development of the science of fracture mechanics deals with linear elastic plane-strain conditions which generally apply to ship hull structures, and b) the loading of ships is of a random nature by virtue of the various influences of cargo loading, sea conditions, ambient temperature, and operating parameters.

The studies of fracture mechanics and of fatigue under random load merge together in the study of crack propagation. This is particularly appropriate with regard to ships since the initiation and growth of cracks is a continuing phenomenon, and since knowledge of growth rates and allowable growth limits is essential in planning for service limitations and timely repair. More basically, such knowledge could be factored into new designs so that any problems of crack formation and propagation could be minimized.

Over the past several years a large amount of data on crack-growth rates under constant stress amplitude or uniformly-varying stress amplitude conditions have been generated. Thus, there is a large bank of data on crack-growth rates versus stress-intensity range, ΔK, for many materials and conditions. Cracks growing under varying amplitudes of stress intensity introduce variations in the material conditions in the region of the crack tip. For example, a large tensile excursion will create a residual compressive stress just beyond the crack tip in many materials. The presence of this residual compressive stress reduces the rate of crack propagation for a number of cycles after the high excursion. The retardation of crack growth depends upon a number of material factors and loading factors which are only partially understood at the present time. Several theories or empirical expressions have been proposed to describe such behaviors. Among such expressions which are of current interest are those of Wheeler (1) and Willenborg (2). Extensions or modifications have been proposed by Morman and Dubensky (3) and Gray and Gallagher (4, 5).

The phenomenon of retardation is of particular interest here since there are indications (ABS 1975 Recommendations for Needed Structural Research) that retardation effects are quite active in ship crack growth. Thus, in order that more accurate predictions of growth rates can be made, it becomes necessary that the retardation phenomenon be quantified directly as it applies to ship and marine structural materials and conditions.

This investigation was intended to provide information on how cracks grow under the typical random loading conditions experienced by ships, and to provide a model which can be used to predict crack-growth behavior. It was concerned only with the effect of applied loads on crack growth. Environment, geometry, and crack initiation were not considered.

Understanding random-load crack-growth behavior is important, since previous studies on other materials and loading conditions have shown that classical methods of predicting crack growth may be conservative, depending upon loading conditions. Eventually, information developed in this program, when combined with studies on crack initiation, environmental effects, and fracture toughness of ship structural steel, can be used to assess the conservatism of existing structural design rules.

1.3 Project Plan

The investigation was conducted by dividing the total project into a number of tasks. These were:

I. Review and Synthesis of Existing Ship Data

II. Definition of Fatigue Loading Spectra

III. Assessment of Fatigue Crack-Growth Retardation

IV. Correlation of Load Spectra with Ship Crack-Growth Experience

A fifth task, concerning the assessment of safety factors, was deleted partway through the program.

1.4 Summary of Results

The characteristics of a "typical" hull bending stress signal were developed through consideration of the various types of loadings.

It was found that the shipboard sequence of stress cycles following an overload, as opposed to aircraft flight profiles, for example, is random, and that no particular pattern emerges as a candidate for use in material characterization.

The data from the TES experimental program show that the average crack-growth rates in two ship structural steels, HY-80 and CS, under variable- amplitude random loading and constant-amplitude loading, agree closely when da/dn is plotted as a function of the root mean square of the stress-intensity range (ΔK_{rms}). Thus, within the limits of this investigation, random and constant-amplitude crack growth can be described by the following equation:

$$da/dn = C(\Delta K_{rms})^m$$

where C and m are material constants.

The random loading sequences used were taken from actual ship loading data obtained by TES from prior investigations. While the overall stress level applied to the specimen was increased in order to cause cracking, the cycle-by-cycle load sequence remained unchanged. Further, modelling of crack-growth behavior also used the identical spectra experienced by the test specimens.

The data also show that crack retardation does result from two short-term loadings experienced by the SEALAND McLEAN. (No attempt was made to represent other ships or to model the long-term distribution). That is, crack growth predicted (using a conventional fracture-mechanics approach by summing the incremental crack extensions occurring in each cycle) is faster crack growth than that actually observed experimentally.

High-frequency, low-amplitude components of the loading spectrum (resonant "whipping" first-mode vibrations due to impulsive loading) had no significant effect on crack-growth rate except insofar as extreme stress ranges are affected. Filtering the signal to remove the high-frequency components (and adjusting the gain to maintain the same total range from lowest trough to highest peak) produced similar crack-growth rates as the unfiltered signal.

2.0 EXPERIMENTAL PROGRAM

2.1 Philosophy

A review of fatigue literature shows that much research has been conducted on the crack-growth behavior of materials under random loading. However, much of this research is not directly applicable to this effort for the following reasons:

1) Subjecting specimens to random loading conditions identical to those seen in service was not possible because:

   a. loading history was not known, or, if known,
   b. mechanical test equipment was not capable of repeating the service load history.

   (As a result, much random loading data comes from "made-up" or simplified spectra more amenable to analysis and machine testing. It is not clear whether any information is lost in the process.)

2) Much data are for Types I and II loading conditions, and are not applicable to Type III loading. (See Section 2.4 for a definition of load types.)

3) Materials investigated were different from those of interest in this program.

Therefore, the philosophy of this program has been to reproduce as nearly as possible in laboratory specimens the actual loading conditions, and to apply a model suitable for those conditions to predict the crack growth occurring in the specimens. The mathematical model would use the same spectra as those applied to the specimens.

In the original development of this investigation, it was hoped that it would be possible to identify actual cracks in ships, and to analyze their growth rate with respect to loading history. However, the practical realities are that cracks are repaired as soon as they become evident, and ship owners are reluctant, for obvious reasons, to publicize their existence. The laboratory experiments with recorded ship data, therefore, are the best substitute for the real thing.

The goals of this test program were to:

1) Demonstrate whether or not crack retardation is occurring in cracks subjected to typical load histories experienced by ships.

2) Develop the crack-growth data resulting from real loading conditions.

3) Demonstrate a suitable model for predicting crack growth under ship loading conditions.

2.2 Selection of a Typical Stress-Time History from Existing Ship Data

For the purpose of the present discussion the total state of stress in a given structural element at a given instant may be classified into the following components:

(a) Local Stress - This includes the locked-in stresses in a structural element which occur during fabrication and assembly as well as the stresses induced by the support of the ship's own structure. The local stress is then the state of stress that exists in the light ship condition. No attempt is made to treat these stresses here since hindcasting the local stresses would be subject to uncertainties of the magnitude of the stress levels themselves.

(b) Initial Mean Stress - The still water bending stress (SWBS) may be induced by the addition of the deadweight which includes cargo, fuel and lube oil, potable water, stores, crew and effects, ballast and light ship bending stress.

(c) Varying Mean Stress - This refers to the stress changes due to deadweight variation and reballasting during the voyage. Fuel burn-off, consumption of consumables, and change in ballasting, all affect the total displacement and attitude of the ship and, consequently, the stresses a structural element may experience.

(d) Stress Due to Ship's Own Wave - This stress is induced by the pressure of the ship's own wave system. Methods are available to estimate the speed dependent bending moment contribution and, thus, the stress contribution from the ship's own wave system.

(e) Diurnal Thermal Stresses - These stresses arise from the thermal expansion of the topside in the day and contraction during the night. The thermal stresses are also affected by the amount of sun exposure occurring during daylight hours.

(f) Low Frequency Wave-Induced Stresses - These stresses are caused by the wave forces on the hull and the ship motions due to these forces. These cyclic stresses occur at the frequency of encounter of the ship with the wave system. The level of stress experienced is directly related to (although not directly proportional to) the significant wave height of the encountered seaway.

(g) High-Frequency Wave-Induced Stresses - These stresses are induced by dynamic wave loads which act on the ship's structure. The most common are bottom slamming, shipping of water on deck, and flare impact. Dynamic loads produce whipping and springing elastic motions of the hull, typically at higher frequencies than the frequency of wave encounter. The impact-induced stresses will produce an initial spike in the stress records followed by high-frequency vibrations.

2.2.1 Data Base

Several ships have been instrumented with gauges by TES for various government and private sponsors. These ships include the HOOSIER STATE, WOLVERINE STATE, MORMACSAN, CALIFORNIA BEAR, BOSTON, UNIVERSE IRELAND, IDEMITSU MARU, ESSO MALAYSIA, FOTINI L., R. G. FOLLIS, and SEA-LAND McLEAN (6). In many cases, measurement of midship bending stress has been the primary data target; and in some cases, measurements have been made at other locations of special interest. Of these ships, the S. S. SEA-LAND McLEAN (SL-7), a high-speed containership, has been the most completely instrumented with over 100 sensors installed and profusely documented (7-10). Therefore, this ship has been selected as the primary data base for the development and application of the method described in this report.

The stress data used to illustrate the method developed here were inferred from the midship longitudinal vertical bending strain gauges. The midship longitudinal vertical bending strain data is derived from an electrically averaged signal obtained from port and starboard strain gauges located on the main deck of the SEA-LAND McLEAN (SL-7). At this time the midship longitudinal vertical bending stress is the only data that has been reduced and presented in a form that is suitable for the present analysis. The methodologies may also be applied to strain data obtained from gauges at other locations if this information is available.

The stress time histories for the SL-7 have been recorded by TES in twenty-minute intervals and presented in various components. The pertinent data summary sheets are shown in Figures 1 and 2. This information is the basis on which the method described herein was developed.

In the context of this report the term load spectra is used as a general term to indicate the loading schedule that would be used as input to a fatigue analysis. Several methods were examined for developing load spectra of various different forms. The data base consists of stress information which has been inferred from analog strain signals. More specifically the load spectra developed herein refer to stress time histories that can be used as input to fatigue crack-growth analysis and long-term statistical stress distributions for use in long-term fatigue analysis. Although the load spectra do not represent loads that occur on the ship per se, they do represent the state of stress that must occur at a given location on a specimen undergoing fatigue testing.

Bending moments may also be inferred from the full-scale strain information. The bending moment information would be representative of the loading incurred by the ship's hull girder at the same location where the strain was measured. This type of presentation is useful in comparisons between different types of ships. It was originally hoped that, given the inferred bending moment at a specified location along the length of a ship, the bending moment and hence the state of stress could be estimated at other locations where strain information was not recorded. However, it does not appear that the methods involved would warrant the quality of results associated with estimating the bending moment or stress at locations other than those where strain information has been recorded.

There are several problems associated with the use of the SL-7 data. First, there is no information available on the state of stress in any of the hull structural elements at the time the strain gauges were installed and it appears that any attempts to hindcast this state of stress would be subject to uncertainties of the magnitude of the stress levels themselves. A second difficulty arises from the fact that strain gauges and associated instrumentation cannot produce reliable data with regard to long-term changes in mean stress. Thus, there is no way in which the mean stress in each structural element at the time of departure from port may be inferred from the measurements. However, the state of stress upon departure may be approximated for the voyages where loading information is available.

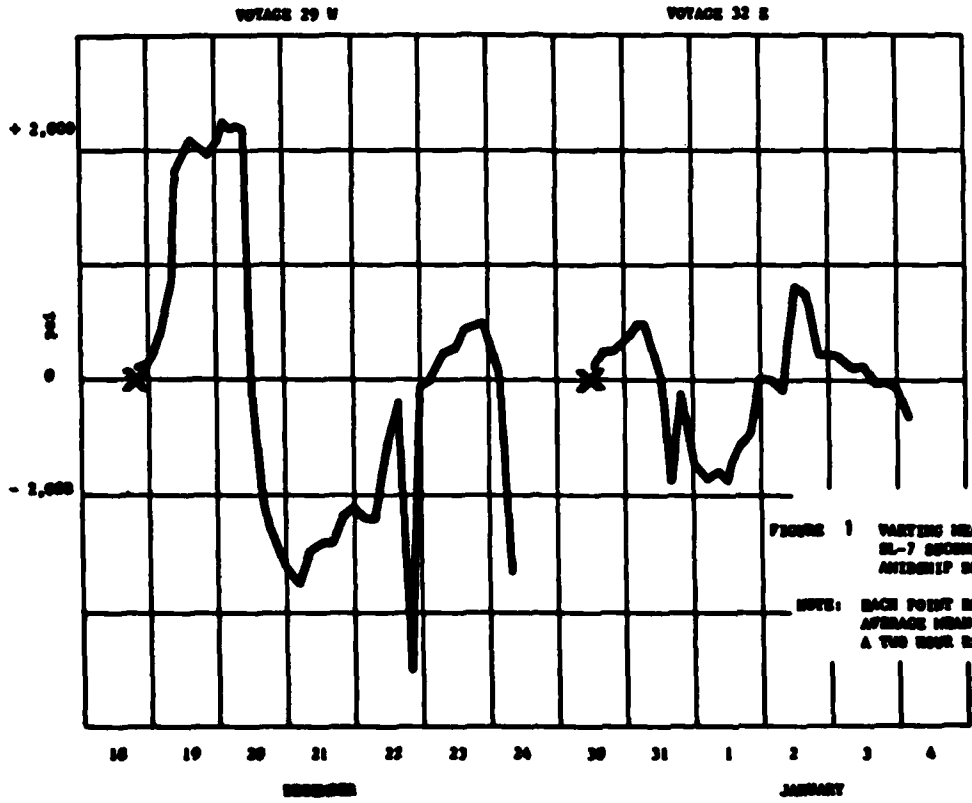

FIGURE 1 VARYING HEAD STRESS
SL-7 SECOND SEASON
ANTHROP SENSING

NOTE: EACH POINT REPRESENTS
AVERAGE HEAD STRESS FOR
A TWO HOUR RECORDING PERIOD

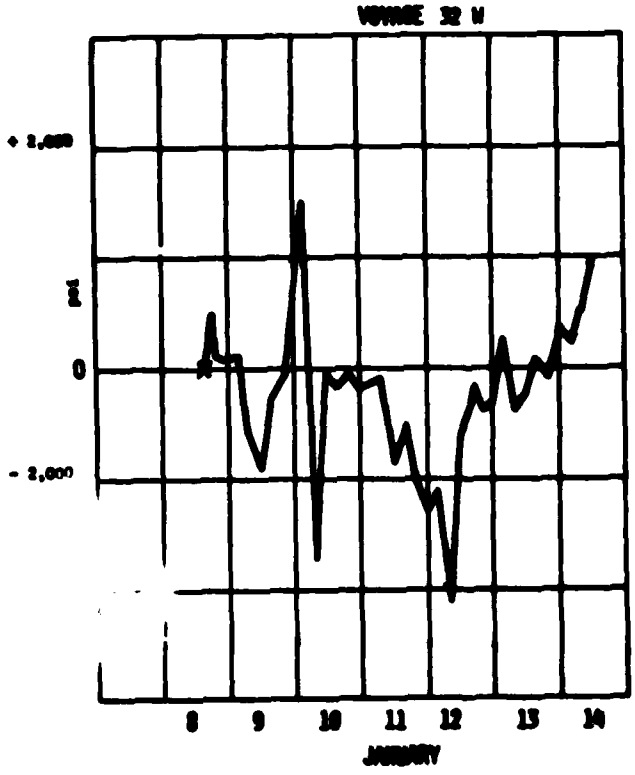

FIGURE 2 VARYING HEAD STRESS.
SL-7 SECOND SEASON.
ANTHROP SENSING.

NOTE: EACH POINT REPRESENTS THE AVERAGE
HEAD STRESS FOR A TWO HOUR RECORDING
PERIOD

2.2.2 Generic Method for Fatigue Load Spectrum Development

The method presented in this report is oriented primarily toward existing ship stress data. However, the method can also be applied to ships during the design stage. The method for arriving at the representative long-term statistical distribution of stresses for ships in the design stages is based on the use of a series of analytical techniques which are currently available. Each type of load may be estimated by the analytical techniques and then combined into a long-term statistical distribution.

The initial and varying still water bending moment may be considered together for computational predictions. In an analytical design study several loading conditions would be determined from expected cargo and routes and the varying mean stress would be calculated as it varies from the initial mean stress.

The basic techniques for calculating the mean stress are well known but are voluminous and time-consuming if done by hand. The simplicity of the equations, however, is one of the reasons for the availability of programs for use in design. For example, the SHCP (Ship Hull Characteristics Program) code applicable to the calculation of the still water bending stress is generally a set of sub-programs which perform the hydrostatic and longitudinal strength calculations. (11)

The wave pattern that is generated as a ship proceeds at an appreciable speed may cause a hogging or sagging moment that is dependent on the ship's hull characteristics. Systematic model tests have been conducted by Vossers (12) and indicate the trend of bending moments over a range of block coefficients and speeds.

The thermal stresses are calculated in two distinct steps: (1) estimate the magnitude of the effect under different conditions of sun exposure; and (2) estimate the frequency of occurrence of these different conditions in service.

Jasper's method (13) can be used to calculate thermal-induced stresses in the weather deck. A reasonable probability function of thermal stress variation can be constructed based on the percentage of time that the sun shines for each temperature variation on the route in question.

Data for such predictions are given in the U. S. Navy Marine Climatic Atlas of the World, Volume VIII (14). The frequency of occurrence of cloud cover for the world's oceans is presented for each month of the year. The cloud cover is then related to air-deck temperature difference by assuming that the insulation ΔT is proportional to the extent of cloud cover. Thermal stresses of a different source may also occur as in the case of LNG carriers.

The most common types of computer programs employed in low-frequency wave-induced stresses are the frequency-domain simulations.

Response amplitude operators (RAO's) for vertical bending moment, lateral bending moment and torsional moments must first be calculated. These RAO's must be computed for a range of wave lengths and headings.

Ships operating in oblique seas are subjected to unsymmetrical bending, so that the stresses measured at one deck edge will usually exceed the mean value. This diagonal bending moment in an oblique sea can be combined by utilizing a method presented in Reference (11).

The next step is to calculate the bending moment response to different sea conditions and then derive a probability density function and a long-term cumulative distribution of bending moments.

The family of sea spectra which are to be used for prediction of wave-induced loads must be selected. If a particular ocean route or routes are to be used, then in general the family of spectra will be based on tabulated data on frequency of occurrence of different combinations observed wave height (significant) and period (average).

Two well-known computer programs available for the above computations are the SCORES and MIT Seakeeping programs. These are frequency-domain ship motion and loads programs accessible to the public domain.

SCORES was developed under SSC Project SR-174, and the MIT Seakeeping program was developed for the U. S. Maritime Administration. Though the basic equations of motion for both programs are identical, their scope is somewhat different. SCORES can handle all six degrees of freedom while the MIT program can simulate only five (surge is excluded). SCORES calculates the vertical and lateral loads as well as torsional moments while the MIT program has been validated over a wide range of ship speeds, wave angles, wave lengths and loading conditions as well as hull form. The agreement between the SCORES calculations and experimental data is generally very good.

Transient high-frequency wave-induced stresses result from hydrodynamic impacts on the ship's structure. The impact loading is generally most severe in the forward portions of a ship's structure where relative velocities between ship and sea are the highest. Energy absorbed from the wave impacts is dissipated through the structure in the form of a dynamic response known as whipping.

The dynamic stresses cannot be considered independently of the structural response of the hull since the response depends on the natural frequency of the hull and on damping from the structure and hydrodynamic environment.

Another important source of high-frequency hull loading is springing. Springing results from the excitation of hull natural modes by the direct action of waves whose frequencies coincide with the hull natural frequencies. This phenomenon occurs commonly in Great Lakes carriers and other ships with similar length to depth ratios.

2.2.3 Stress-Time History Selection

This section presents a method for selecting a typical stress-time history from the SL-7 data base to be used in the experimental portion of this study.

The length of the selected stress-time history is limited to the twenty-minute interval for several practical reasons. Although it would be desirable to conduct a fatigue test or an analytical simulation for an entire voyage, the fatigue testing approach chosen by TES for this program is limited by the length of signal which can be effectively fed to the testing machine and by cost considerations. The stress-time histories as recorded are broken down into components of mean stress, wave-induced stress, and burst data. In this methodology, each component is analyzed separately, and from each component a most probable value of occurrence of the ship's lifetime is then recreated. After the representative stress value is calculated for each stress element, it is then possible to enter the summary sheets and select an existing stress interval with the characteristics calculated by using the proposed technique. The development and results of the representative value for each stress element or component are presented next.

As stated in Section 2.2.1, the strain gauges were reset to zero upon departure for each voyage. However, loading conditions, displacements and trims permitted estimation of the initial mean stress. It was originally hoped that several representative loading conditions could be analyzed, but time and cost considerations precluded a statistical estimate of the initial mean stress. Instead, a single departure loading condition was obtained for the voyage 32w and the still water bending stress was calculated by ABS using a ship hydrostatics program. Another source of initial mean stress data was the loading condition existing at the calibration voyage from Reference 15.

Although there are limitations involved in determining the initial mean stress, it seems reasonable to consider the 32w voyage as being typical of the SL-7 operation. Both stresses were calculated using standard beam equations given the resultant bending moment from the loading conditions. The calculated initial mean stresses, for the 32w and calibration voyages are 6481 psi and 6251 psi, respectively.

The varying mean stress which results from the burn-off of consumables and ballast changes appears to be random in nature. Figures 3 through 6 show plots of the varying mean stress for several voyages. The representative or typical value for the varying mean stress would be the average of the available data. The varying mean stress does not appear to be related to weather encountered by the vessel. Furthermore, there appear to be no parameters associated with the varying mean stress that would facilitate the ratio and extrapolation to a period beyond which measured data have been recorded.

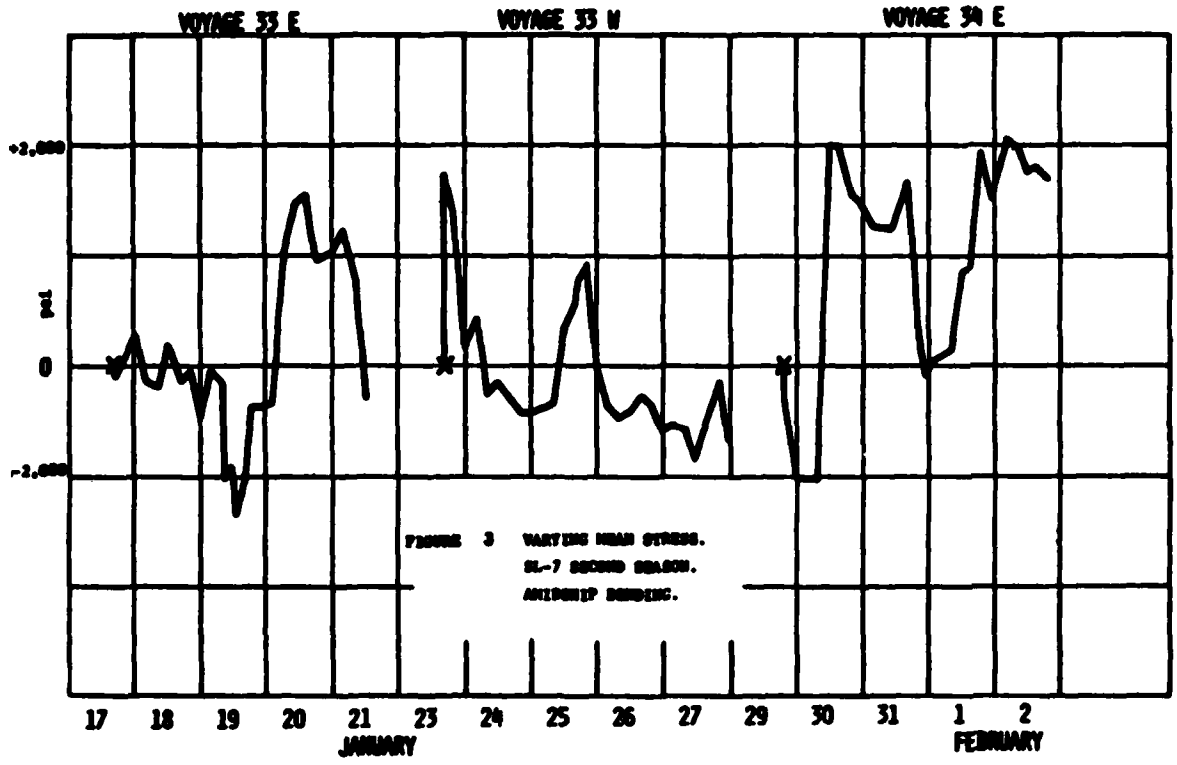

FIGURE 3 VARYING HEAD STRESS.
SL-7 SECOND SEASON.
ASHDOWIP BENDING.

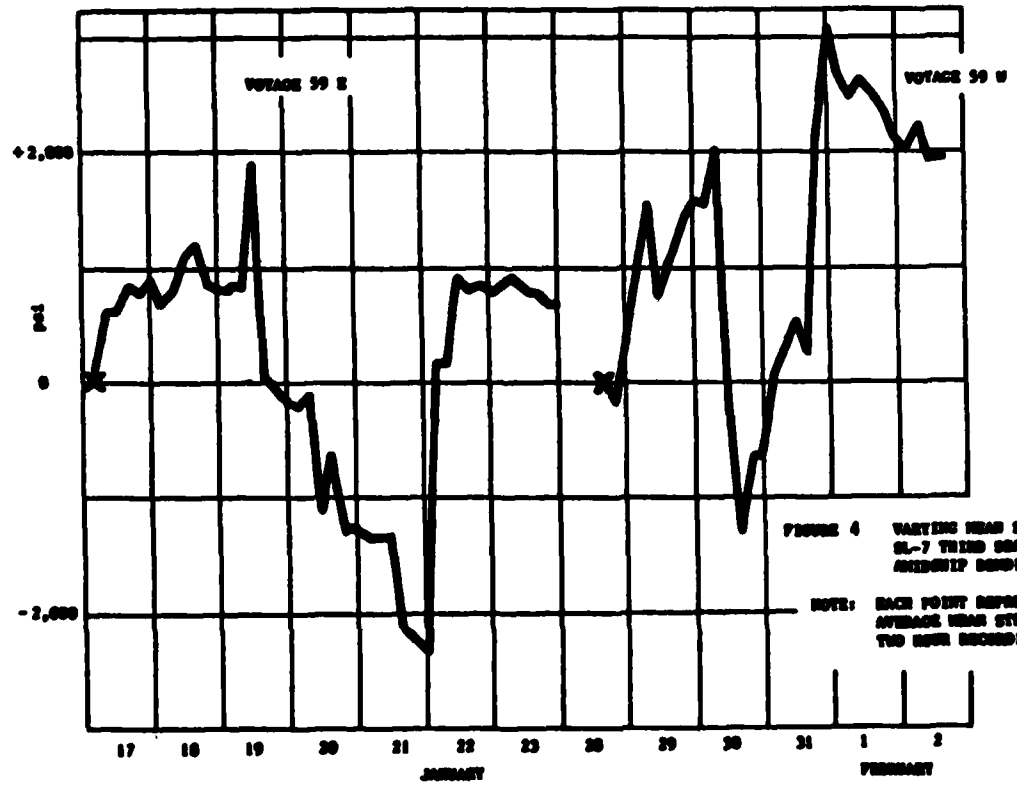

FIGURE 4 VARYING HEAD STRESS
SL-7 THIRD SEASON
ASHDOWIP BENDING

NOTE: EACH POINT REPRESENTS THE AVERAGE HEAD STRESS FOR A TWO HOUR RECORDING PERIOD.

SUMMARY TAPE MCLEAN 1973-1974 SEASON MIDSHIP VERTICAL BENDING CHANNEL 1

ANALOG TAPE NUMBER	LOGBOOK INDEX NUM	DATE	LATITUDE	SHIPS COURSE	PROP RPM	REL WIND DIR	REL WAVE DIR	WAVE PD SECS
TRIP	INTERVAL NUM	TIME GMT	LONGITUDE	SHIPS SPEED KTS	SEA STATE	REL WIND SPEED KNOTS	WAVE HT FEET	WAVE LENG FT
MCLEAN143 32W	005 017	01-08-74 2000	51-39 N 002-07 E		• 07	035P 45	035P 10	
MCLEAN143 32W	005 018	01-08-74 2000	51-39 N 002-07 E		• 07	035P 45	035P 10	
MCLEAN143 32W	005 019	01-08-74 2000	51-39 N 002-07 E		• 07	035P 45	035P 10	
MCLEAN143 32W	005 020	01-08-74 2000	51-39 N 002-07 E		• 07	035P 45	035P 10	
MCLEAN143 32W	006 021	01-08-74 2400	51-39 N 002-07 E	233 30.5	123.7 07	008P 40	008P 10	
MCLEAN143 32W	006 022	01-08-74 2400	51-39 N 002-07 E	233 30.5	123.7 07	008P 40	008P 10	
MCLEAN143 32W	006 023	01-08-74 2400	51-39 N 002-07 E	233 30.5	123.7 07	008P 40	008P 10	
MCLEAN143 32W	006 024	01-08-74 2400	51-39 N 002-07 E	233 30.5	123.7 07	008P 40	008P 10	
MCLEAN143 32W	007 025	01-09-74 0400	51-39 N 002-07 E	233 32.5	131.6 06	149S 30	149S 08	
MCLEAN143 32W	007 026	01-09-74 0400	51-39 N 002-07 E	233 32.5	131.6 06	149S 30	149S 08	
MCLEAN143 32W	007 027	01-09-74 0400	51-39 N 002-07 E	233 32.5	131.6 06	149S 30	149S 08	
MCLEAN143 32W	007 028	01-09-74 0400	51-39 N 002-07 E	233 32.5	131.6 06	149S 30	149S 08	
MCLEAN143 32W	008 029	01-09-74 0800	51-39 N 002-07 E	233 32.5	131.9 09	104S 40	104S 12	
MCLEAN143 32W	008 030	01-09-74 0800	51-39 N 002-07 E	233 32.5	131.9 09	104S 40	104S 12	
MCLEAN143 32W	008 031	01-09-74 0800	51-39 N 002-07 E	233 32.5	131.9 09	104S 40	104S 12	
MCLEAN143 32W	008 032	01-09-74 0800	51-39 N 002-07 E	233 32.5	131.9 09	104S 40	104S 12	

FIGURE 5

SUMMARY SHEET FOR S.S. SEA-LAND McLEAN VOYAGE 32 W

SUMMARY TAPE MCLEAN 1973-1974 SEASON MIDSHIP VERTICAL BENDING CHANNEL 1
PAGE 698

REL SWELL DIR	SWELL LENGTH FEET	SEA TEMP	WEATHER	SWELL HT FEET	BAROM INCH HG	AIR TEMP	MAX P-TO-T STRESS PSI	NUMBER OF BURSTS	COMMENTS	NUMBER CYCLES	RMS STRESS PSI ---HAVE IND---	MAX STRESS PSI 1ST MODE	MEAN STRESS PSI
035P	0400	E	OCAST	010	29.66	039				188	9146 3623	37 2114	UACK IN AUTO OPERATION 208
035P	0400	E	OCAST	010	29.66	039				188	8809 3914	38 2696	BACK IN AUTO OPERATION 191
035P	0400	E	OCAST	010	29.66	039				176	6931 4159	51 2451	BACK IN AUTO OPERATION 298
035P	0400	E	OCAST	010	29.66	039				186	12187 4312	59 4534	BACK IN AUTO OPERATION -269
008P	0400	E	PT CLDY	010	29.63	038				179	9044 4297	48 4534	222
008P	0400	E	PT CLDY	010	29.63	038				171	12187 4879	58 4573	206
008P	0400	E	PT CLDY	010	29.63	038				163	12861 5002	61 4980	282
008P	0400	E	PT CLDY	010	29.63	038				171	10839 4473	50 3830	-338
014S	0500	E	OCAST	010	29.38	041				164	8579 3707	17 2481	176
014S	0500	E	OCAST	010	29.38	041				164	6717 3094	12 1907	237
014S	0500	E	OCAST	010	29.38	041				167	8227 3194	18 2206	306
014S	0500	E	OCAST	010	29.38	041				164	10011 3623	25 2062	-261
104S	0500	E	CLDY	010	29.76	050				179	6924 4098	50 2880	MOD 10 HEAVY PITCH -621
104S	0500	E	CLDY	010	29.76	050				188	9023 3799	51 3807	MOD 10 HEAVY PITCH -514
104S	0500	E	CLDY	010	29.76	050				178	8870 3878	50 3247	MOD 10 HEAVY PITCH -452
104S	0500	E	CLDY	010	29.76	050				187	7943 3761	44 3094	MOD 10 HEAVY PITCH -927

FIGURE 6

SUMMARY SHEET FOR S.S SEA-LAND McLEAN VOYAGE 32 W

The low-frequency wave-induced stresses, which are directly related to the wave heights encountered by the ship, are presented in the TES summary sheets (see Figures 5 and 6) in the form of an RMS value for each twenty-minute interval. In addition each interval has an associated observed wave height which is recorded and presented in the summary sheets. The interpretation of the observed wave height in order to derive a significant wave height is difficult to do. It is assumed that by grouping the wave heights and RMS stresses into categories, the wave height representation will be adequate.

The general plan for development of a typical RMS wave-induced stress is to average the RMS values for each of several wave height categories and then calculate a weighted average RMS based on the frequency of occurrence of the wave heights over the ship's lifetime. The RMS stresses are averaged for each of six wave height groups from the second season and one-half of the third season. The average RMS stress values for the corresponding wave height are shown in Figure 7. Although these stresses are obtained from the second and third seasons, they can be combined into a weighted average based on the frequency of occurrence of the wave heights expected over the ship's lifetime. The frequency of occurrence for each wave height group is obtained from Reference 16 and presented in Table I. The weighted average RMS stress, calculated as indicated above, becomes 3021 psi as indicated in Table II.

The high-frequency wave-induced stresses can also be related to the observed wave height and weighted average can be developed based on the occurrence of the wave heights for the ship's lifetime.

Although it was originally hoped that the typical high-frequency component would be derived from the long-term distribution of high-frequency stresses, the information is not available at this time.

The high-frequency wave-induced stresses are presented in the summary sheets as burst data and a single maximum peak-to-trough stress for each twenty-minute interval.

A typical number of bursts were estimated per interval for the high-frequency wave-induced stresses, utilizing the same techniques as for the low-frequency wave-induced stress information.

Although the burst data is less dependent on the encountered wave height than the low-frequency wave-induced stresses, the encountered wave height or sea condition is the only relevant parameter presented for each interval.

The number of bursts for each interval was developed from a weighted average. The average number of bursts per wave group is shown in Figure 8. The frequency of occurrence for the six wave groups is shown in Table II. The typical number of bursts expected for the ship's lifetime is 18 bursts/interval.

FIGURE 7 AVERAGE RMS STRESS VS. OBSERVED WAVE HT. (AMIDSHIP BENDING STRESS)

- - - - ONE-HALF THIRD SEASON

——— SECOND SEASON

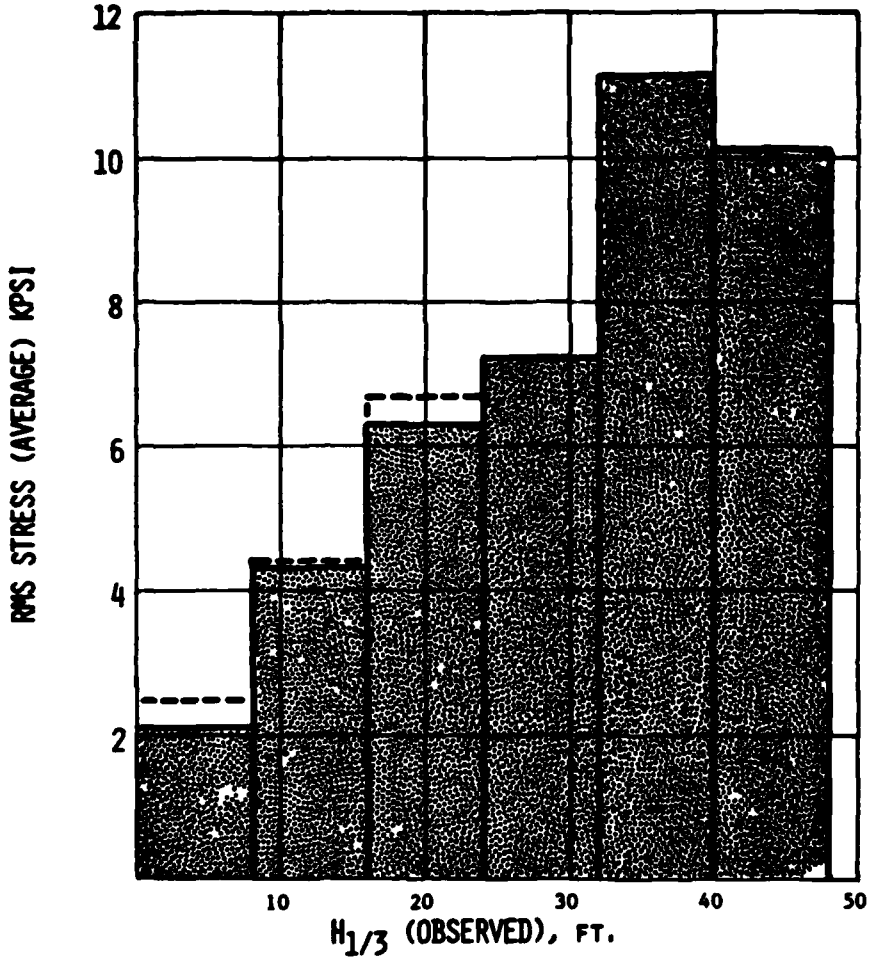

FIGURE 8 NUMBER OF BURSTS/INTERVAL VS. OBSERVED WAVE HEIGHT FROM SECOND SEASON DATA

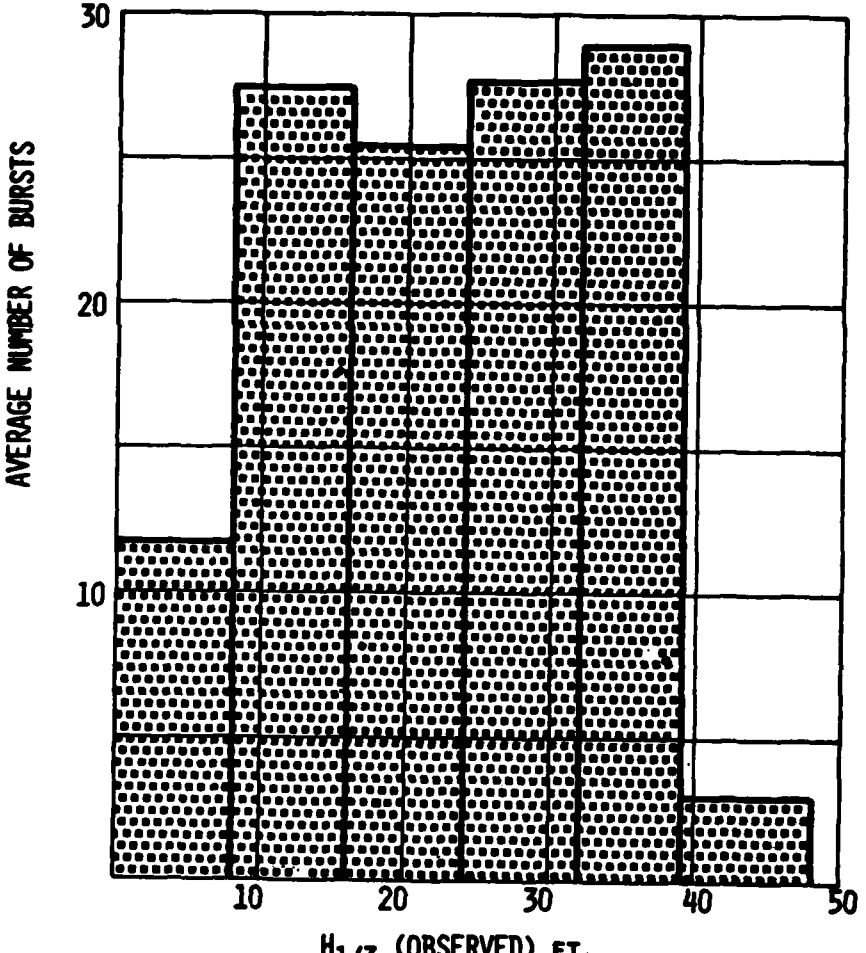

TABLE I

Average RMS Stress
Based on Probability of Occurrence
For Each Wave Group

Wave Group	Probability of Occurrence of Wave Group	Average RMS Stress KPSI	Product of Probability of Occurrence of Wave Groups and Average RMS Stress
I	.6294	2.037	1.282
II	.3133	4.320	1.353
III	.039	6.325	.247
IV	.0167	7.249	.121
V	.0012	11.093	.0133
VI	.0004	10.694	.0043

Total of Products = 3.021 KPSI

TABLE II

NORTH ATLANTIC ROUTING - WAVE OCCURRENCE PROBABILITY

$H_{1/3}$ (ft.)	WAVE GROUP	% OCCURRENCE
0-8	I	62.92
8-16	II	31.33
16-24	III	3.9
24-32	IV	1.67
32-40	V	0.12
40-50	VI	0.04

Summarizing the results, the representative values for each stress component become:

(a) Initial mean stress: 6,481 psi
(b) Varying mean stress: 167 psi
(c) Low-Frequency Wave-Induced stress (RMS): 3,021 psi
(d) High-Frequency Wave-Induced stress: 18 bursts/interval

Given this information, it is possible to synthesize or construct a stress signal for crack-growth analysis using the techniques presented previously. However, a signal may be selected from the stresses recorded on the SL-7 SEA-LAND McLEAN containership which closely fits these characteristics. This typical signal may be chosen from summary sheets similar to those shown in Figures 5 and 6.

2.3 Fracture-Mechanics Approach to Crack Growth

In linear elastic fracture mechanics, the stress field at the tip of a crack is described in terms of stress intensity with a function of the following form:

$$K = F\ \sigma\sqrt{a}\ (\text{Ksi}\sqrt{\text{in}})$$

where σ = gross stress (Ksi)
a = crack length (in)
F = geometry correcting factor, dependent upon crack and part geometry

In the literature there exist stress-intensity solutions for a wide variety of crack shapes and loading cases.

The stress intensity is used in all known schemes for calculating crack-growth rates. For constant-amplitude crack growth, it has been shown that crack growth is a function of ΔK where $\Delta K = (K_{max} - K_{min})$. That is: $da/dn = f(\Delta K)$.

When constant-amplitude crack-growth rate (da/dn) is plotted against ΔK on log-log paper, an S-shaped curve results, as shown in Figure 9. Traditionally, this curve is broken into three regions, called Stage I, II, and III crack growth. Stage I crack growth, sometimes called threshold crack growth, applies when crack-growth rates are very low. Small changes in ΔK substantially alter the crack-growth rates. Stage II crack growth (sometimes referred to as steady-state crack growth) is characterized by a nearly linear relation between log da/dn and log ΔK, while Stage III crack growth is characterized by a rapidly increasing crack-growth rate and results from crack instability.

Several models have been presented which attempt to describe the relation between da/dn and ΔK. The simplest, and limited strictly to Stage II crack growth, is the Paris equation:

$$\frac{da}{dn} = C(\Delta K)^m$$

where C and m are material-dependent, and are determined by experiment. Other relations account for stress ratio effects, or include Stage I or Stage III crack growth.

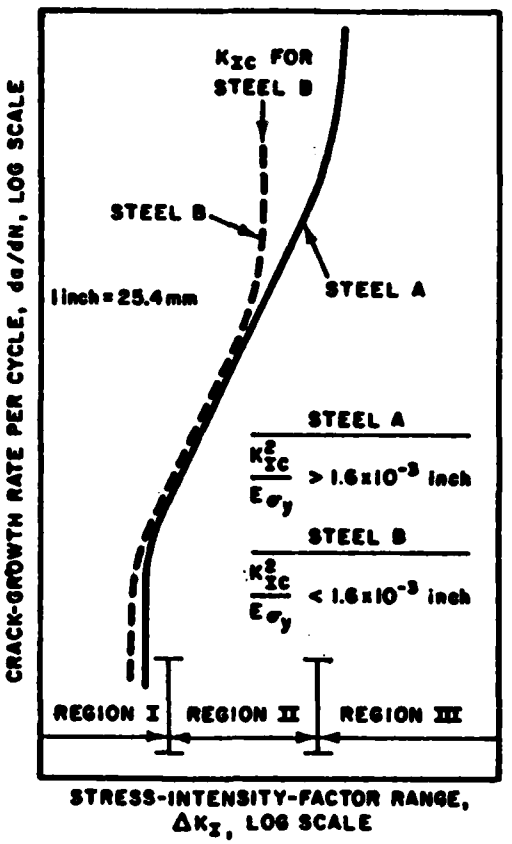

Figure 9 Schematic representation of crack growth in steels

2.4 Random Loading

Traditionally, crack-growth investigations have been conducted with constant-amplitude, constant-frequency loading spectra. This has been sufficient when structures designed from such data really experience such spectra in service, or when such data is used to compare the relative crack-growth characteristics of a variety of materials. However, many structures are subjected to essentially random loading conditions in service. There are three basic types of random loading spectra:

1) Constant-amplitude spectrum with random spike overload or underload (Type I).

2) Constant-amplitude block loading spectrum, wherein the spectrum consists of a series of blocks, each block being of constant amplitude (Type II).

3) Truly random variations in load (Type III).

Different models have been developed, usually based on some constant-amplitude relation modified to predict crack growth for random loading. Each type of model is designed for a particular type of loading spectrum. It is generally not possible to apply a model developed for one specific loading condition to another loading condition without modification of the spectrum.

The need for specialized models for random loading conditions arises from the fact that when the relation for constant amplitude loading is applied to predict random loading crack growth, the crack-growth rate predicted is substantially faster than is actually observed. This slower observed crack growth is the result of crack retardation. This phenomenon is well documented in the literature, and several theories are available to explain this behavior (17). The extent of crack retardation can be assessed by comparing measured crack lengths in specimens subjected to a random load signal with the crack length predicted from conventional fracture mechanics, assuming no retardation is occurring.

2.5 The Root-Mean-Square Stress Intensity Model

One model which has been used successfully in the past for predicting Type III random loading crack-growth behavior is the Root-Mean-Square Stress-Intensity Model (18), abbreviated here as ΔK_{rms}. This model is based on the Paris equation, with ΔK replaced by ΔK_{rms}:

$$\frac{da}{dn} = C(\Delta K_{rms})^m$$

where C and m are the material-dependent constants which are determined from constant-amplitude tests. In constant-amplitude tests, $\Delta K_{rms} = \Delta K$. Therefore, this model predicts that if da/dn data from random loading tests are plotted against ΔK_{rms}, the same result should be obtained as for da/dn data plotted against ΔK from constant amplitude tests. The method of determing ΔK_{rms} is described in 3.5 of this report.

2.6 Experimental Procedures

2.6.1 Materials

Two materials were used in this test program, HY-80 and an ABS grade, CS. The mechanical properties of each are presented in Table III.

2.6.2 Specimens

1.0 T Compact Specimens machined in accordance with ASTM E-647 requirements were produced from plate stock. All specimens were from an L-T orientation. A typical specimen is shown in Figure 10.

2.6.3 Constant-Amplitude Tests

Constant-amplitude crack growth measurements were made for both materials over a range of stress intensity ratios (R values) at R = 0.05, 0.30 and 0.60. The range of R values was incorporated to assure that R value did not have a large effect on crack-growth rate, since the model does not have any provisions to consider the effect of R.

All constant-amplitude tests were run in accordance with ASTM E-647 requirements. Initially, crack lengths were determined two ways simultaneously: visual observation of crack length on the surface of specimen, and measurement of specimen compliance (19). In the latter, crack-opening displacement on the end of the specimen can be correlated with crack length. Eventually, sufficient confidence was developed in the compliance method so that only spot visual checks of crack length were made. All data reported here resulted from compliance measurements.

Crack length versus time data were converted to da/dn versus ΔK using the seven-point incremental polynomial method described in ASTM E-647. The test environment was laboratory air, with no control of humidity. Test temperature was nominally $70^{o}F$, $\pm 5^{o}$.

2.6.4 Random Loading

Specimens subjected to random loading were tested identically to the constant-amplitude specimens with the exception that a random load was substituted for the constant-amplitude spectrum.

2.6.5 Random Loading Spectra

The random loading spectra consisted nominally of 25 minutes of actual as-recorded ship loading data, increased in speed 25 times, and recorded on a one-minute loop cassette. Output from a cassette player was used to drive the closed-loop servohydraulic test machine in place of the conventional function generator. The amplitude of the random signal was adjusted so that the specimen always experienced a tensile load. (The compact tension specimen is not suitable for compression testing; i.e., an R value less than zero.) Thus, the specimen was subjected to the actual dynamic load sequence recorded from ship loading. The same data was repeated continuously until fracture of the specimen occurred. Ideally, a greater length of recorded loading history would have been used to cut down the number of repetitions. However, difficulties in handling the increased amount of data would have resulted, and the one-minute tape loop was selected as a compromise between ideals and experimental realities.

TABLE III

Mechanical Properties of Materials Used in Test Program

	HY-80	CS
Tensile strength, psi	110,400	66,450
Yield strength, psi	86,100	45,500
Reduction in area, %	59	66
Elongation, %	21	33

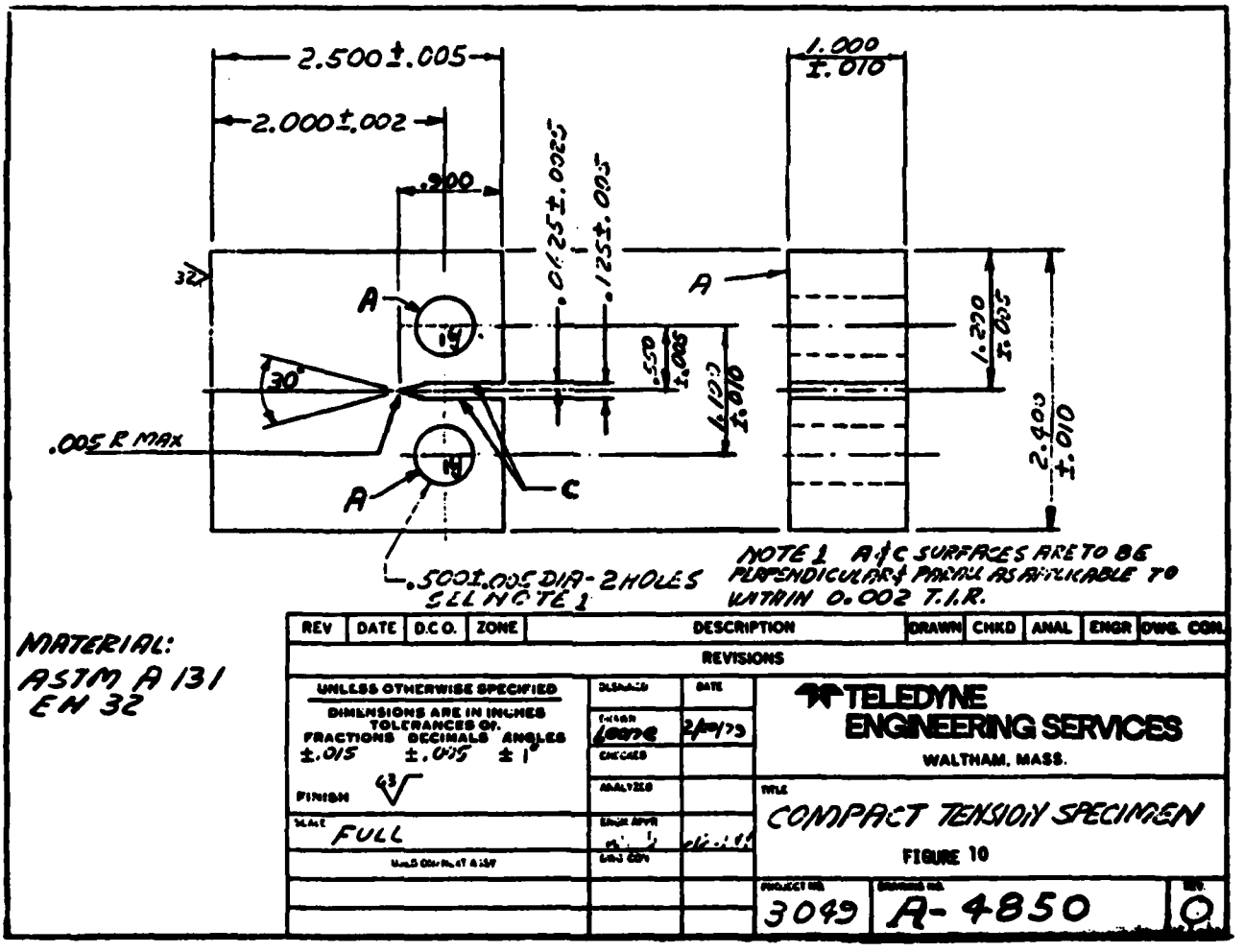

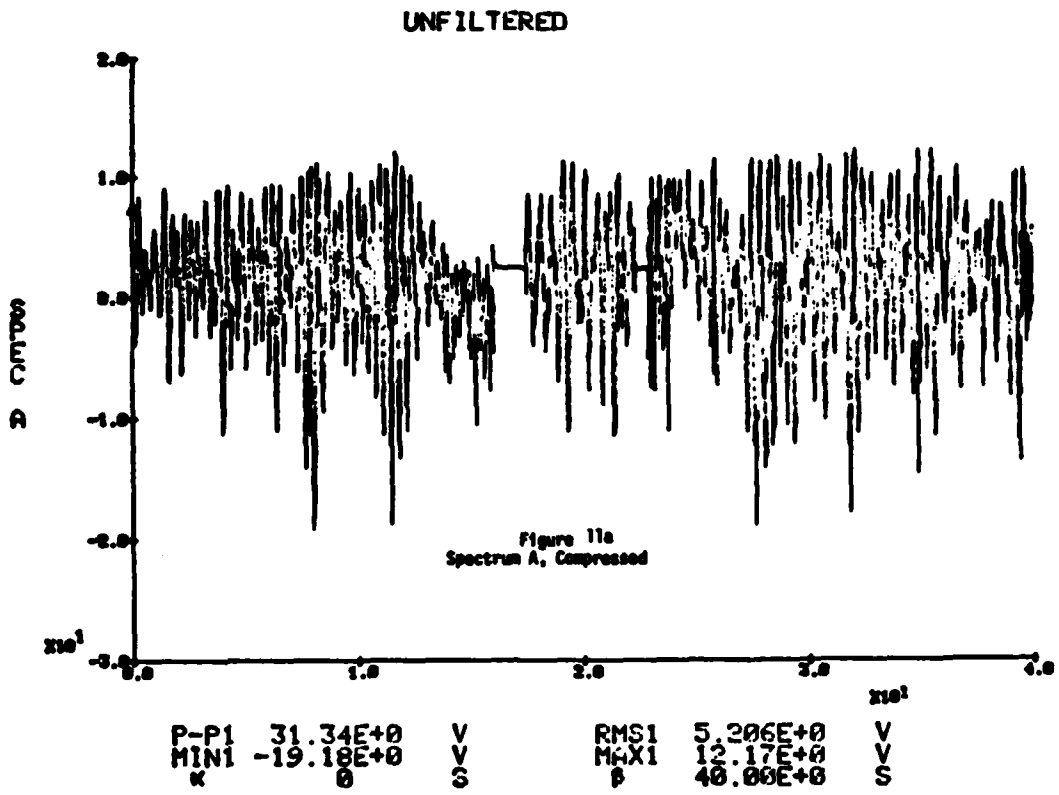

Figure 11a
Spectrum A, Compressed

P-P1	31.34E+0	V	RMS1	5.206E+0	V
MIN1	-19.18E+0	V	MAX1	12.17E+0	V
α	0	S	β	40.00E+0	S

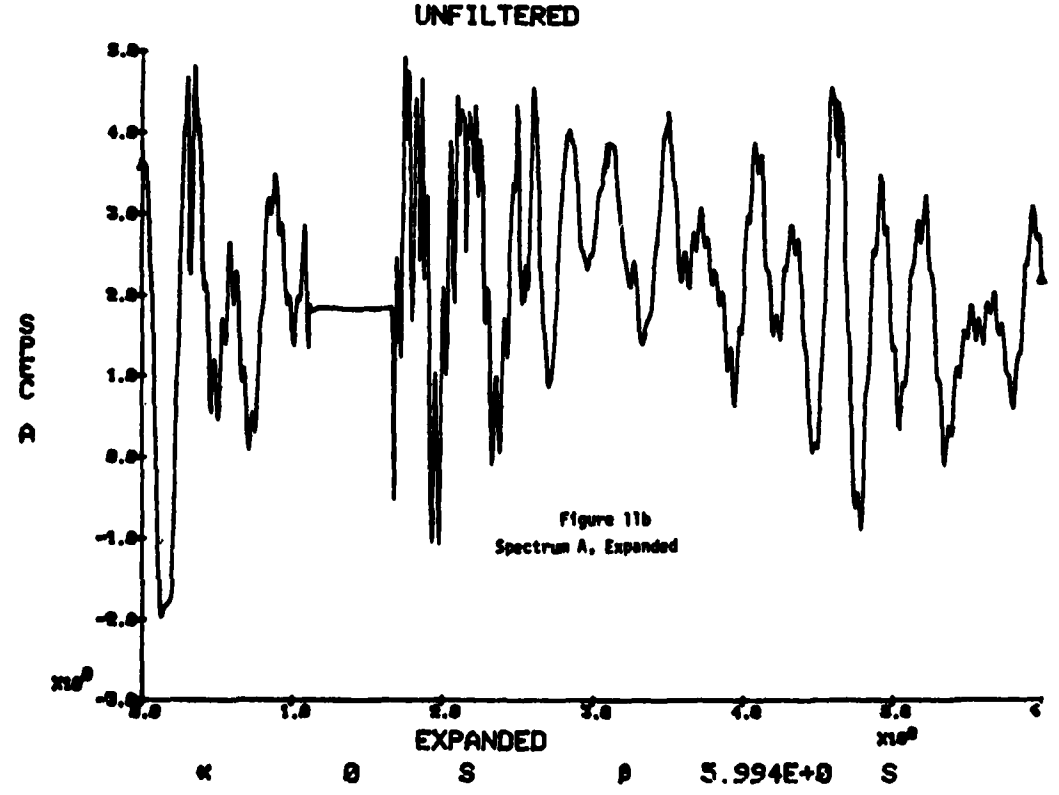

Figure 11b
Spectrum A, Expanded

α	0	S	β	5.994E+0	S

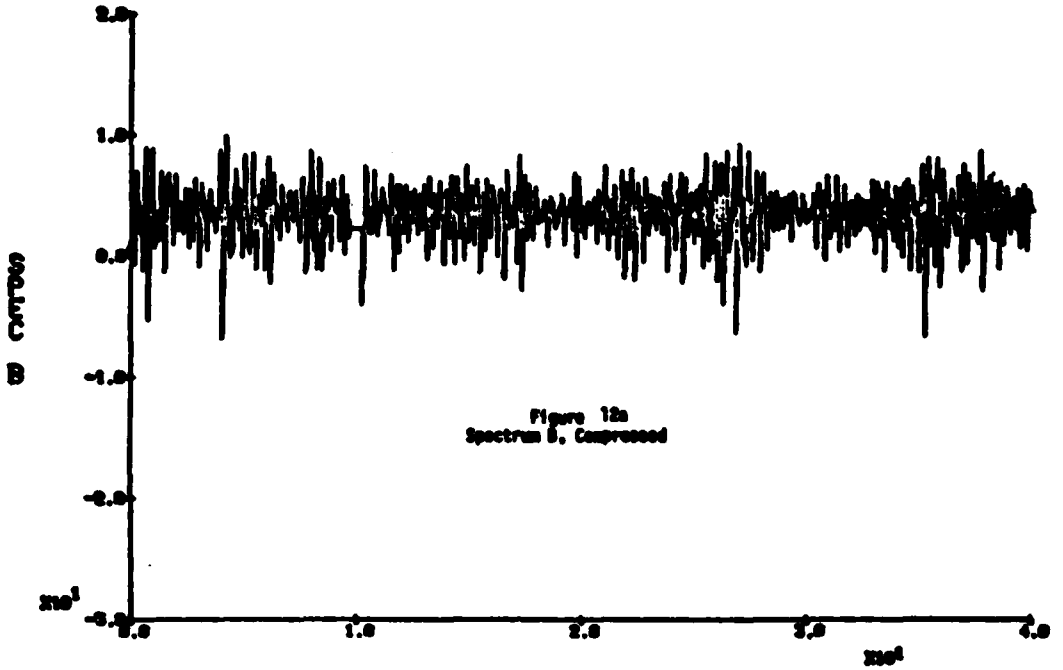
UNFILTERED
Figure 12a
Spectrum B, Compressed
P-P1 16.69E+0 V
MIN1 -6.815E+0 V
α 0 S
RMS1 3.942E+0 V
MAX1 9.873E+0 V
β 40.00E+0 S

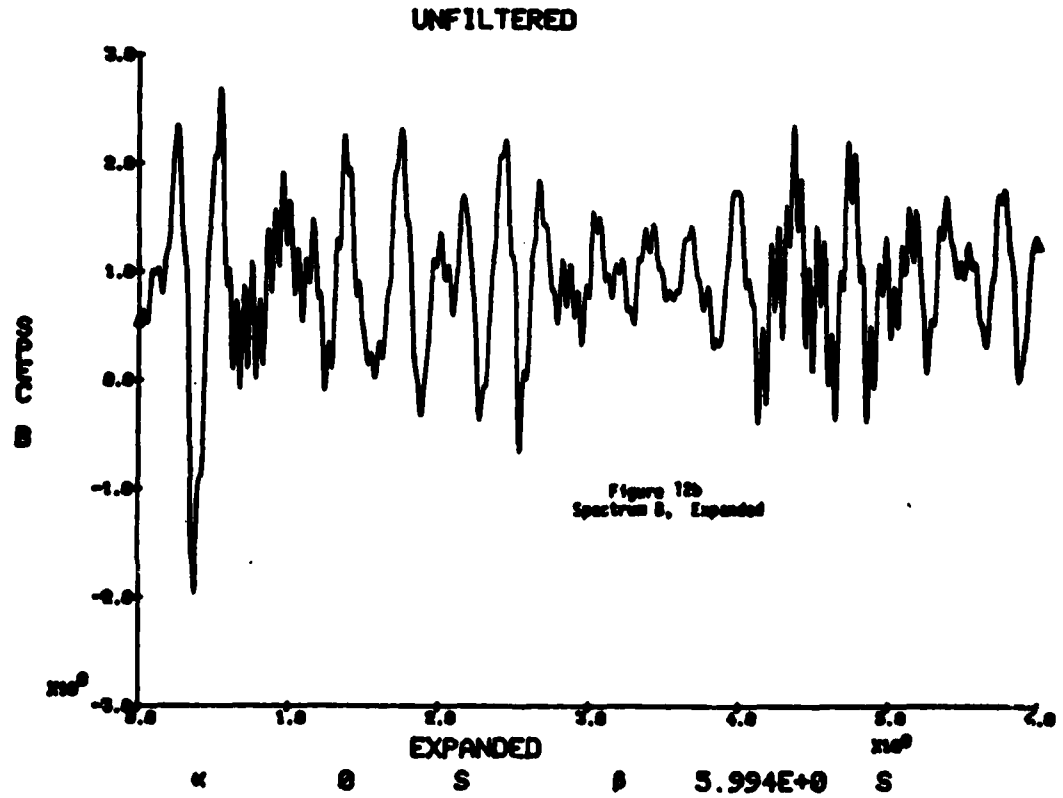
UNFILTERED
Figure 12b
Spectrum B, Expanded
EXPANDED
α 0 S
β 5.994E+0 S

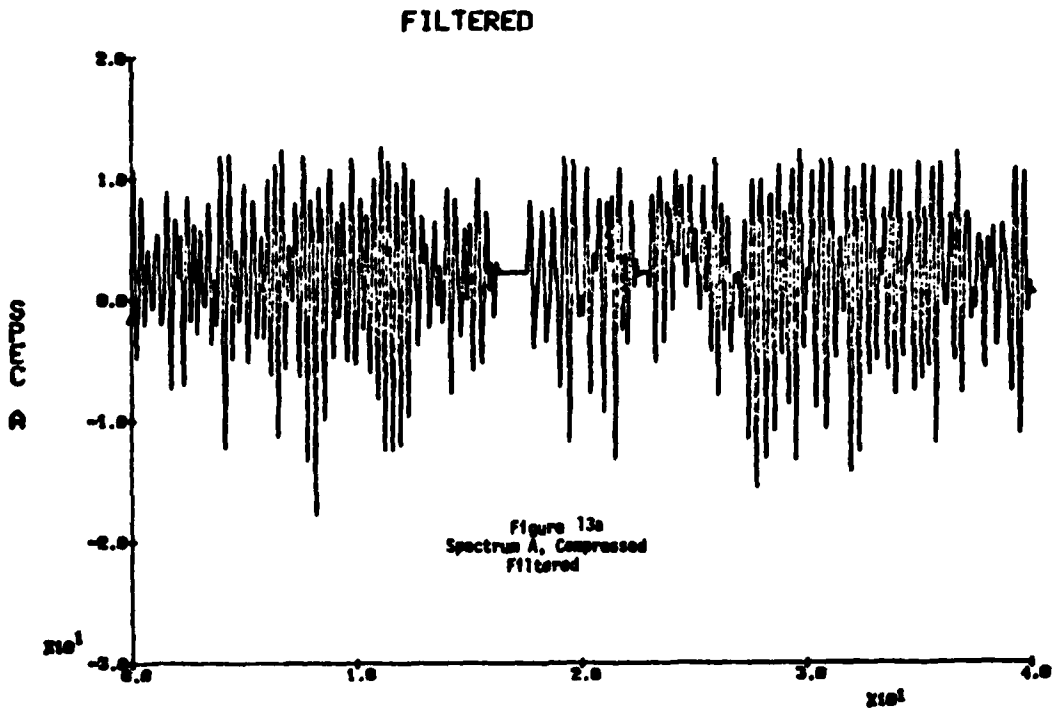

Figure 13a
Spectrum A, Compressed
Filtered

P-P1	30.36E+0	V	RMS1	5.697E+0	V
MIN1	-17.81E+0	V	MAX1	12.55E+0	V
α	0	S	β	40.00E+0	S

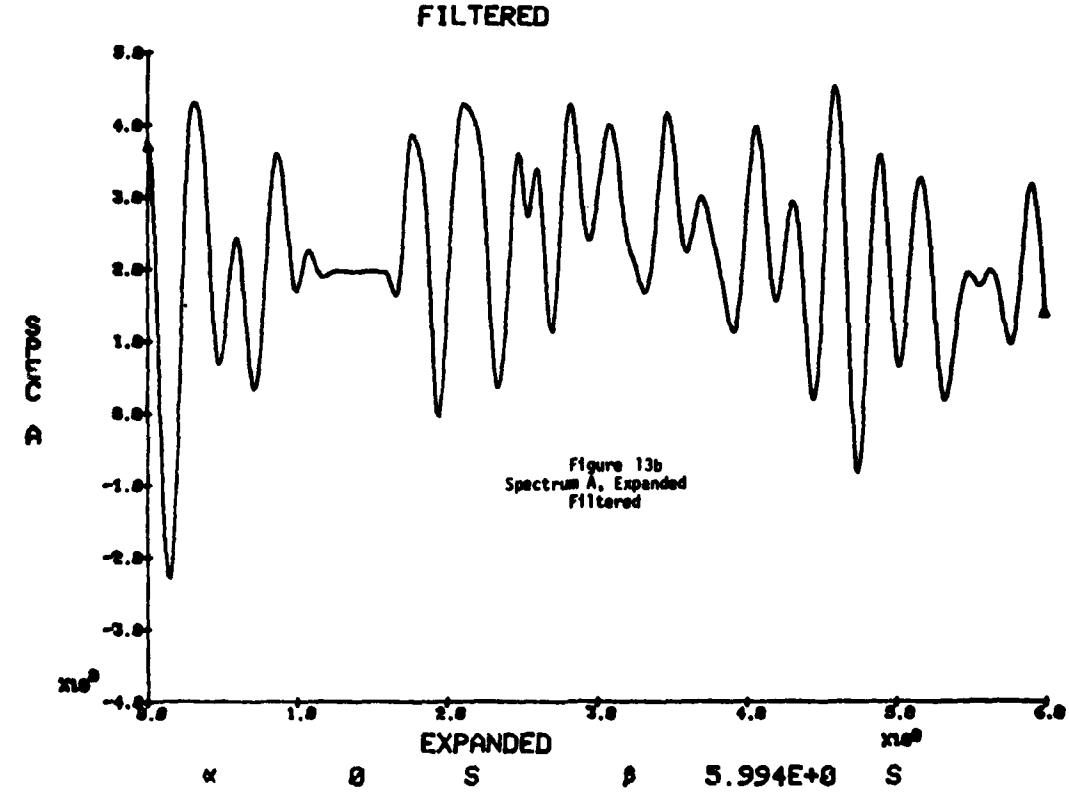

Figure 13b
Spectrum A, Expanded
Filtered

α	0	S	β	5.994E+0	S

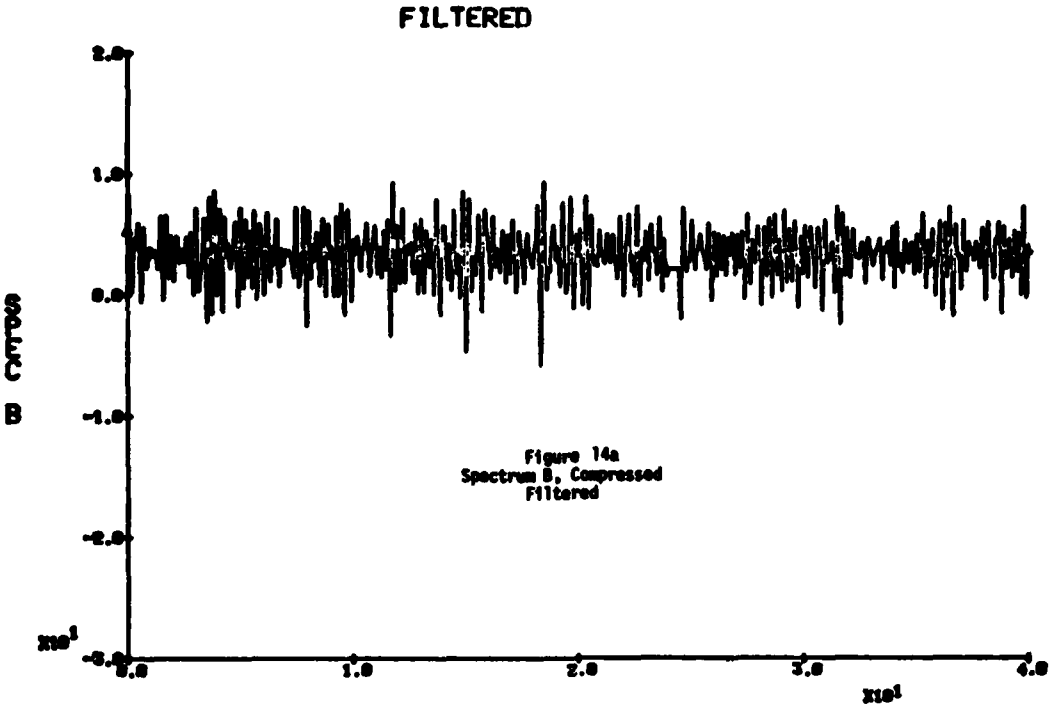

Figure 14a
Spectrum B, Compressed
Filtered

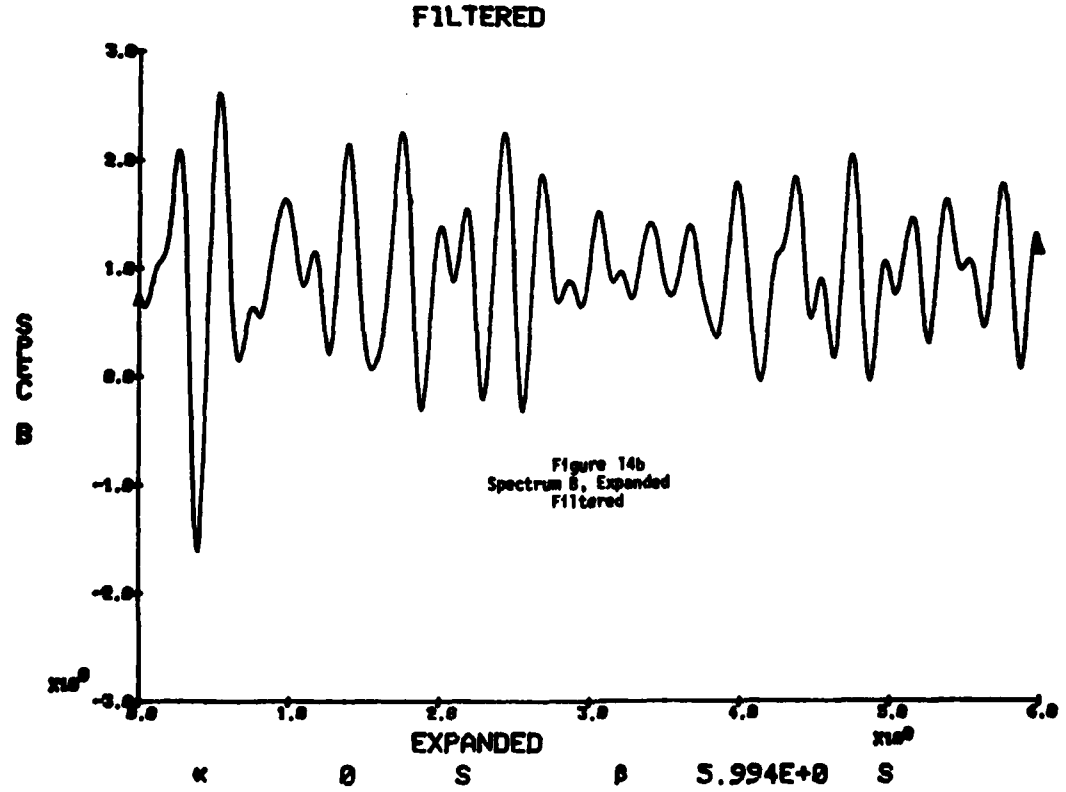

Figure 14b
Spectrum B, Expanded
Filtered

The loading spectra used were taken from data recorded by TES from strain gages placed aboard the SS SEALAND McLEAN. Two spectra were used, identified as:

Spectrum A:	Spectrum B:
Tape 145	Type 143
Voyage 32W	Voyage 32W
Interval 018	Interval 021
01-11-74 1200 GMT	01-08-74 2400 GMT

Load versus time records for portions of these two spectra, compressed and expanded in time, are shown in Figures 11 and 12. These spectra have characteristics essentially as determined by GAA in Section 2.2.3 of this report.

In addition to subjecting the specimens to the actual as-recorded spectra, for some tests each spectrum was passed through a filter to remove the high-frequency vibration component resulting from wave impacts. Typical records of the filtered spectra are shown in Figures 13 and 14. The high-frequency component, at about 1 Hz, is the first-mode vibrational beam bending of the hull. The low-frequency component is directly wave induced, and has a frequency between 0.1 and 0.075 Hz. These two signals superimpose, and result in time histories like those of Figures 11 and 12. Thus, these spectra should be distinguished from the purely random "white noise" type of signal. By filtering, the discrete high-frequency portion of the spectrum is removed.

In order to visualize the effect of filtering on the appearance of the spectra, compare Figures 11B and 13B or 12B and 14B, which are the unfiltered and filtered versions of the same sequences of spectra A and B. Note that there are fewer cycles in the filtered spectra and as a result of removal of the high-frequency components, the magnitude of the filtered versions may be slightly lower.

2.6.6 Crack-Length Measurement

In constant-amplitude tests, the specimen is loaded at a constant frequency. This allows examination and measurement of crack lengths visually using a strobe to "stop" the crack. In random loading, the frequency is varying constantly; thus, the strobe is out of phase with the maximum loads, and the tip of the crack is difficult to see. Therefore, crack-length measurement is more difficult in specimens subjected to random loading.

Compliance measurement of crack length is also difficult. With constant-amplitude tests the crack-opening displacement is measured at the point of maximum load during each cycle. The result can be correlated to crack length. For random loading, if the compliance is measured at one of the peaks in a single cycle, the crack-opening displacement measured can be used to calculate a crack length, but that crack length may not be the actual crack length since the phenomenon of crack closure may be present. The crack-opening displacement must be measured during the highest peak in the random cycle. Only at this time can there be any assurance that the maximum crack opening displacement has occurred, and the actual crack length is being measured.

To accomplish this, TES used a PDP-8 computer to monitor crack-opening displacement, by sampling output from the crack-opening displacement gage at the rate of 250 times per second. Periodically, the computer printed out the maximum crack-opening gage reading which had occurred since the last printout. By knowing the maximum load seen by the specimen in the one-minute tape loop, the actual crack length can be calculated.

Details of the experimental setup are shown in Figures 15 through 18.

2.6.7 Experiment Variables - Constant Amplitude

In the constant-amplitude crack-growth experiment, crack length is measured as a function of the number of cycles. R ratio and material are the two variables. The specimens tested with constant-amplitude spectra, their applied loads, and R ratios, are shown in Table IV.

2.6.8 Experiment Variables - Random Loading

In random loading, different variables were considered:

1) There are many ways of counting the number of cycles in a random spectrum. Recognizing that the same spectrum recurs every minute, crack length was measured as a function of time.

2) Two versions of each spectrum were produced: the original, and one in which the signal was passed through a low-pass filter to remove the (realtime) 1 Hz vibration component. The presence or absence of the vibration component, then, is a test variable.

3) R ratio was not considered, since R will vary with each cycle. Rather, for random loading, R was defined as the ratio of the minimum to maximum signal in the entire one-minute tape loop. This value was always set at 0.05.

In order for a crack-growth experiment to be considered valid according to E-647, there are definite limits set on the maximum stress intensity (K_{max}) to which the specimen can be subjected. Increasing R in the random spectrum increases K_{max}, resulting in the K_{max} limitations being exceeded early in the experiment. Thus, little data could be generated in a single specimen. Therefore, R was limited to a single value. Note that, since the amplitude of each filtered spectrum was decreased slightly because of filtering, the signal to the test machine had to be amplified slightly (5%) to maintain the same R and K_{max} as for the comparable unfiltered spectrum.

Figure 15. The TES Random Load Fatigue Crack Growth Test Facility

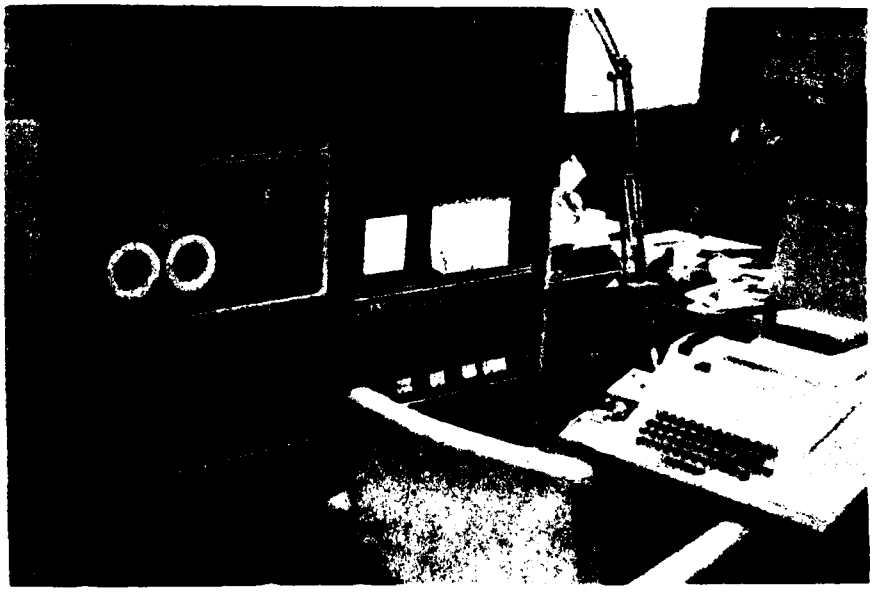

Figure 16. TES PDP-8 Computer for Continuous Monitoring of Random Load Crack Growth

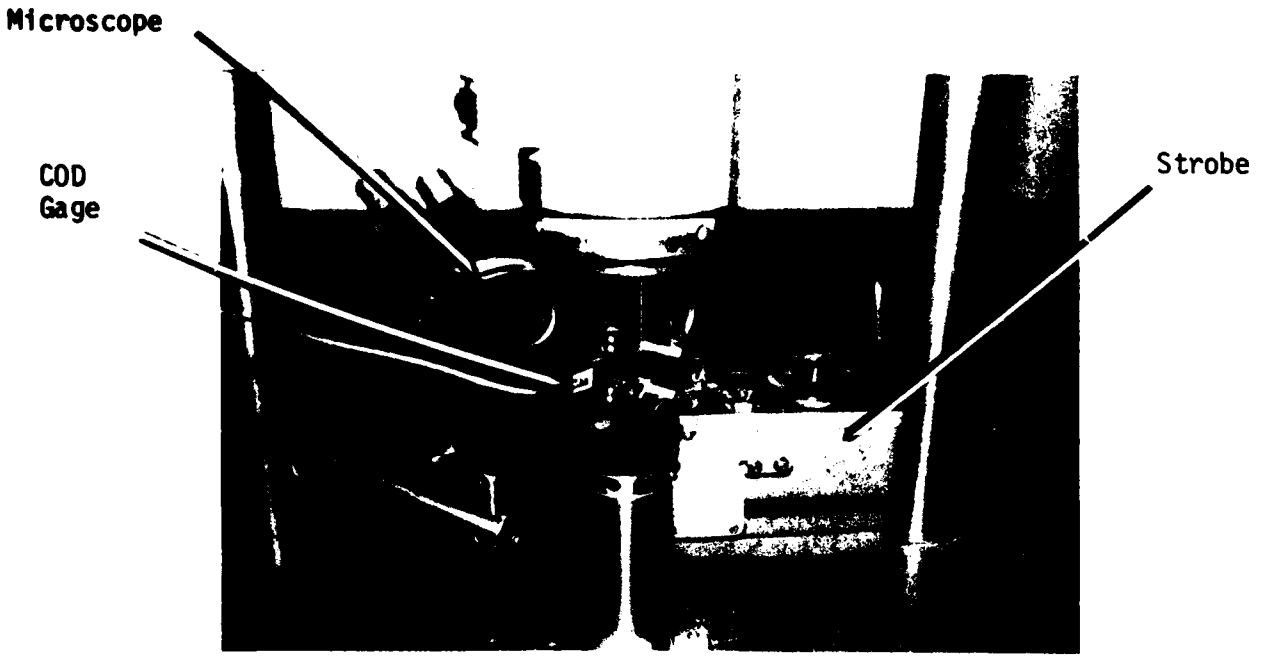

Figure 17. CT Specimen in load frame showing strobe and microscope for visual examination and COD gage for crack length measurement

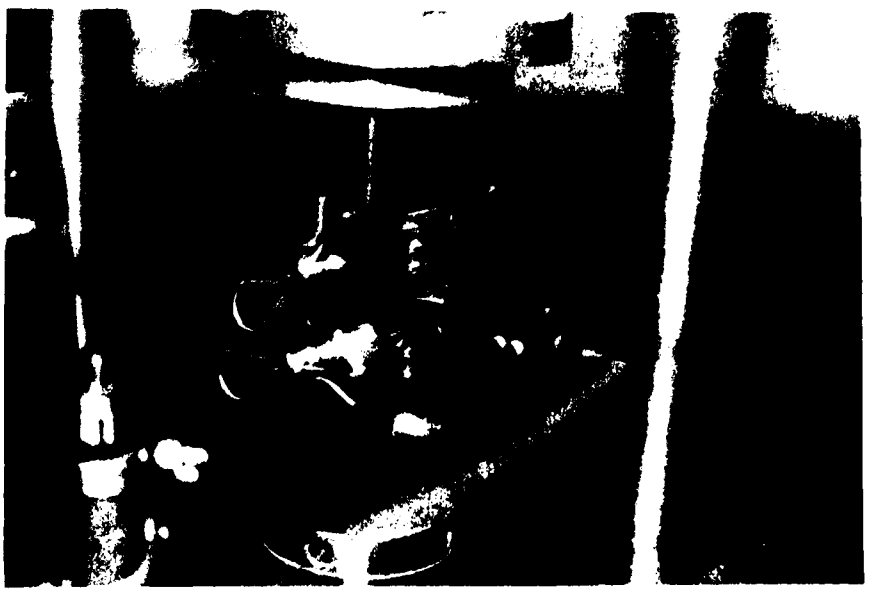

Figure 18. Close-up of CT specimen in grips with attached COD gage

TABLE IV

Specimens Tested and Experimental Variables

Material	Specimen No.	Load, P (pounds) P_{min}	P_{max}	R	Spectrum
HY-80	4	7500	12,500	0.60	Constant Amplitude (CA)
"	5	7500	12,500	0.60	CA
"	6	1240	4,140	0.30	CA
"	9	430	8,700	0.05	CA
"	8	150	2,900	0.05	CA
"	11	3750	12,500	0.30	CA
CS	6	4350	7,250	0.60	CA
"	17	1240	4,140	0.30	CA
"	13	1240	4,140	0.30	CA
"	18	430	8,700	0.05	CA
"	20	150	2,900	0.05	CA
"	8	430	8,700	0.05	CA
HY-80	20	430	8,700	0.05	Random A
"	23	430	8,700	0.05	Random A
"	22	430	8,700	0.05	Random A Filtered
"	27	625	12,500	0.05	Random A Filtered
"	1	625	12,500	0.05	Random B
"	25	625	12,500	0.05	Random B
"	12	625	12,500	0.05	Random A
CS	15	430	8,700	0.05	Random B
"	24	625	12,500	0.05	Random B
"	21	625	12,500	0.05	Random A Filtered
"	10	430	8,700	0.05	Random B Filtered
"	11	625	12,500	0.05	Random B Filtered
"	23	625	12,500	0.05	Random A

The variables in the random tests were, therefore:

1) Material (HY-80 or CS)
2) Filtered or Unfiltered Spectrum
3) Spectrum A or B

Table IV lists the specimens and variables.

3.0 ANALYSIS PROCEDURES

3.1 Philosophy

It was the goal of the analytical portion of this investigation to predict crack growth using a crack-growth model with the actual spectra experienced by the specimens. From the literature (20, for example) it is apparent that many predictions of crack growth are based on modifications to the actual spectrum in order to make the predictions easier to compute. This is satisfactory as long as the test specimen has experienced the same modified spectrum. If not, the crack-growth prediction process may be complicated, particularly if initial results do not satisfactorily predict crack growth, in which case it becomes necessary to determine what portion of the simplification is affecting the prediction. To avoid this potential difficulty, TES used the actual spectrum without modifications to the loading sequence.

3.2 Digitizing

The analog signal from the random load tape loops used to drive the test machine was converted to a digital record using an analog-to-digital converter sampling the analog signal at the rate of 250 times per second. This digital record was the basis for all crack-growth predictions for each spectrum.

3.3 Cycle Counting

For modelling purposes it is necessary to know the actual number of cycles in each spectrum as well as the load levels for each cycle. There are many schemes for counting cycles (21). TES used the following: First, it is assumed that all damage occurs on the loading side of each cycle. The rest of the cycle is not relevant. Next, a cycle is defined as the interval from one stress reversal to the next stress reversal, no matter how small. The method of analyzing the random signal is shown schematically in Figure 19.

The digitized record was sorted according to the above scheme, resulting in a series of numbers alternating between relative load maxima and minima.

3.4 Crack-Growth Prediction Using Conventional Fracture Mechanics

Using conventional fracture mechanics based on the Paris equation, crack growth under random loading is predicted by summing all the increments of crack growth which occur in each cycle, and assuming no retardation occurs.

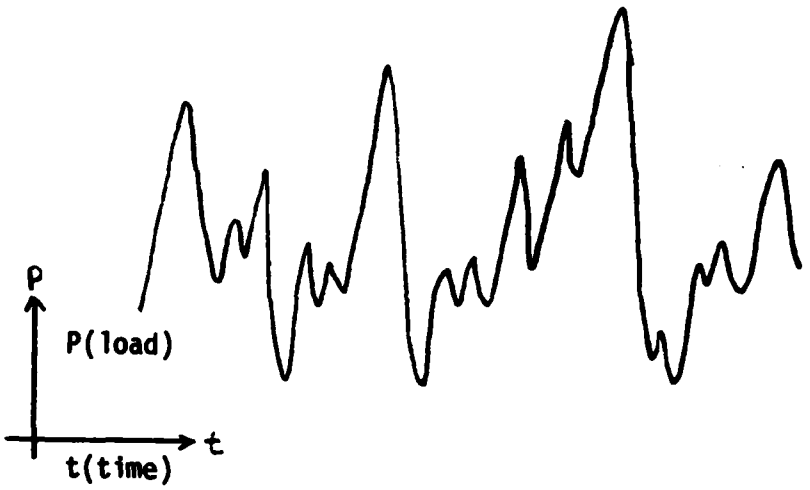

Typical spectrum applied to test specimen

Spectrum after digitizing and conversion of continuous function to straight-line segments joining peaks. Note that even the smallest cycle is retained.

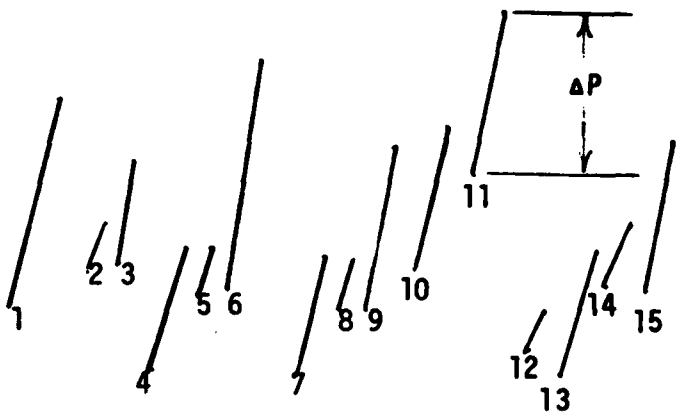

Spectrum as used by model. Only loading portion of each cycle is used. Each cycle has been numbered.

Figure 19

Conversion of actual spectrum to form usable by computer program

This process is described with the following relations:

$$a_n = a_o + \sum_{n=1}^{N} \left(\frac{da}{dn}\right)_n$$

and

$$\left(\frac{da}{dn}\right)_n = C(\Delta K_n)^m$$

a_n = Crack length at cycle n

N = Total number of cycles

a_o = Initial crack length

C, m = Material constants determined from constant-amplitude tests

3.5 Fitting Crack-Growth Rate

In any kind of crack-growth studies, it is common practice to plot da/dn data as a function of ΔK on log-log graphs. The ΔK_{rms} model assumes that random crack-growth data can be plotted as a function of ΔK_{rms}. Since in a constant-amplitude spectrum $\Delta K = \Delta K_{rms}$, the random data plotted against ΔK_{rms} on the same scale as the constant-amplitude data should be the same as the constant-amplitude data.

Random crack-growth data was originally determined in the form of crack length (a) versus time (t). Knowing there are a fixed number of cycles in each minute (for each repetition of the tape loop) and knowing the number of cycles from the cycle-counting procedure, it is a simple multiplication to convert time to cycles. Since ΔP_{rms} remains constant during any test, the random load (a) versus (n) data can be converted to da/dn versus ΔK_{rms} using exactly the same procedures as for constant-amplitude data. That is, da/dn is calculated using the seven point incremental polynomial method of ASTM E-647, and ΔP_{rms} is substituted for ΔP in the equation for calculating ΔK, giving ΔK_{rms}.

4.0 EXPERIMENTAL RESULTS

4.1 Constant Amplitude - HY-80

Constant-amplitude da/dn versus ΔK data are presented in Figure 20. R values tested were R = 0.05, 0.30 and 0.60. A linear least-squares fit to these data gave the following values for (C) and (m) for use in the Paris equation:

$$C = 1.77 \times 10^{-9}$$
$$m = 2.54$$

The threshold stress intensity (ΔK_{th}) was approximately 15 to 16 ksi$\sqrt{\text{in}}$. While determination of ΔK_{th} was not a part of this program, for the purposes of comparing materials and spectra ΔK_{th} is defined here as the stress intensity at da/dn = 1×10^{-6} in/cycle.

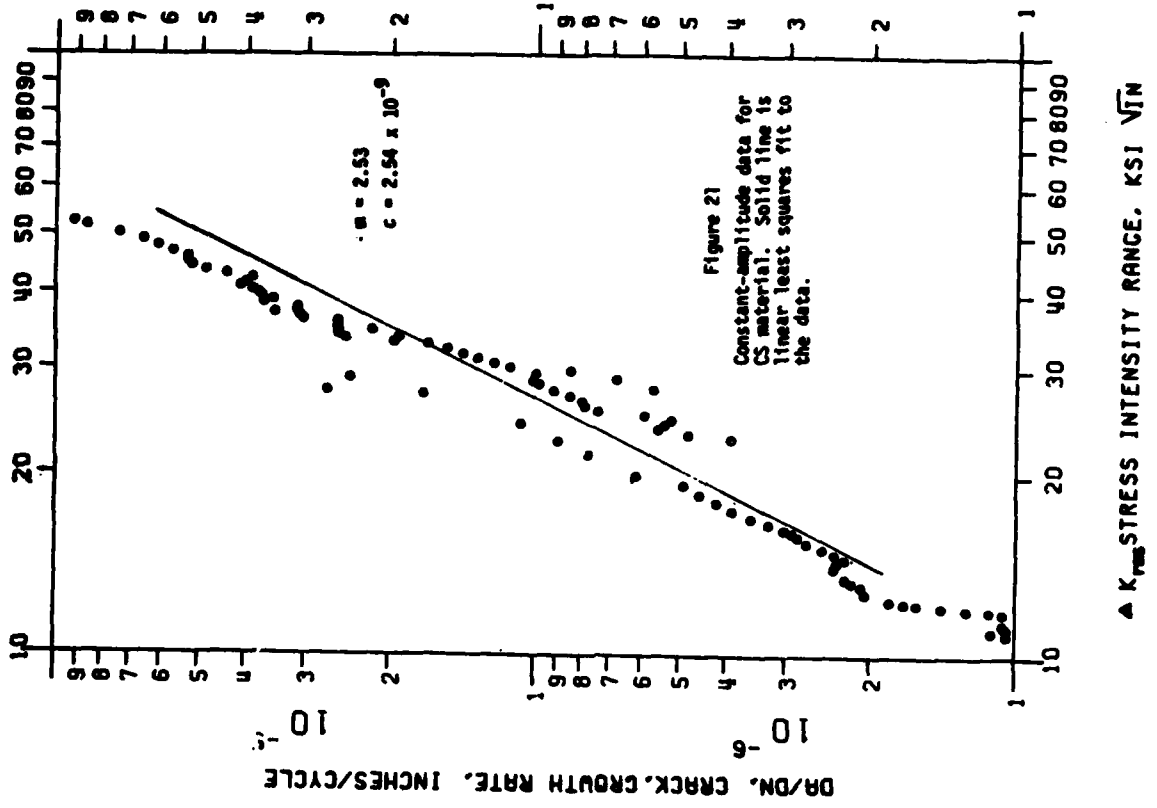
m = 2.53
c = 2.54 x 10⁻⁹
Figure 21
Constant-amplitude data for CS material. Solid line is linear least squares fit to the data.
da/dN, CRACK GROWTH RATE, INCHES/CYCLE
10⁻⁶
10⁻⁵
Δ K_res STRESS INTENSITY RANGE, KSI √IN

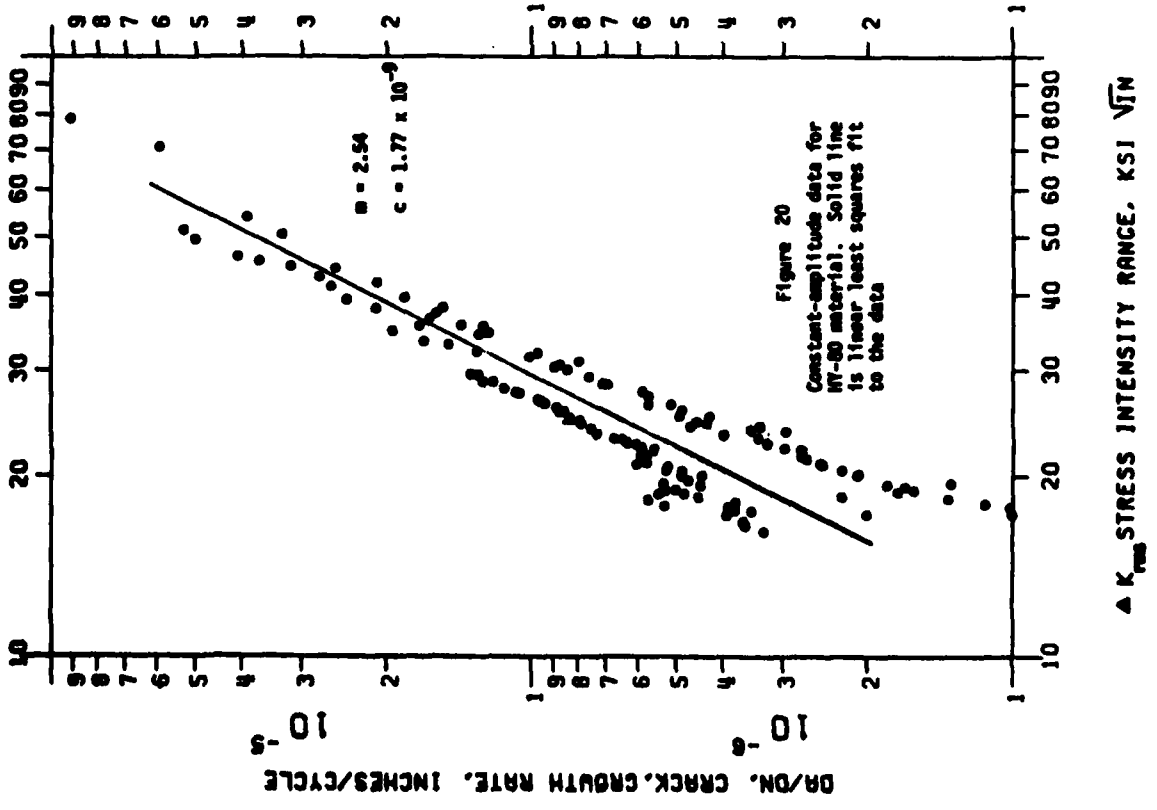
m = 2.54
c = 1.77 x 10⁻⁹
Figure 20
Constant-amplitude data for HY-80 material. Solid line is linear least squares fit to the data
da/dN, CRACK GROWTH RATE, INCHES/CYCLE
10⁻⁶
10⁻⁵
Δ K_res STRESS INTENSITY RANGE, KSI √IN

4.2 Constant Amplitude - CS

Constant-amplitude da/dn versus ΔK data is presented in Figure 21. R values tested were R = 0.05, 0.30 and 0.60. A linear least-squares fit to the data gave the following values for (C) and (m) for use in the Paris Equation:

$$C = 2.54 \times 10^{-9}$$
$$m = 2.53$$

The threshold stress intensity (ΔK_{th}) was approximately 10 to 11 ksi $\sqrt{in}$. (As described in 4.1, ΔK_{th} is defined here as the stress intensity at da/dn = 1×10^{-6} in/cycle). HY-80 was more resistant to crack propagation than the CS material.

4.3 Random-Loading Crack Length Versus Time

Crack growth as a function of time was essentially the same for the filtered and unfiltered spectra when the spectra had the same R values and maximum load and the same initial crack length. This was true for both materials. Figure 22 compares crack growth for two specimens for the same spectrum, one containing high-frequency components, the other filtered to remove them. The fact that the filtered spectrum had faster crack-growth rate may be the result of a 5% amplification of the filtered signal as described in 2.6.8.

Spectrum B produced faster crack growth than Spectrum A for the same R value and maximum load. This is shown in Figures 23 and 24, for example.

HY-80 had better crack propagation properties in random loading, as shown in Figures 25 and 26.

4.4 Random Loading da/dn Versus ΔK_{rms}

Crack growth versus time (a versus t) data for randomly loaded specimens was converted to da/dn versus ΔK_{rms} in the manner described previously in Section 3.5. It was found that the data for the filtered spectra fit well with the constant-amplitude data, but that the specimens with unfiltered spectra had a crack-growth rate approximately one order of magnitude lower than the constant-amplitude data at the same ΔK.

In Section 4.3 it was noted that filtered and unfiltered versions of the same spectrum resulted in approximately the same crack-growth rate as a function of time. When (a) versus (t) data for specimens tested with the unfiltered spectrum were converted to da/dn versus ΔK_{rms} assuming they were tested with a filtered spectrum (i.e., omitting the small-amplitude cycles from the count), it was found that the data agreed with both the constant-amplitude data and the randomly loaded data for specimens subjected to a filtered spectrum.

This observation was true for both spectra A and B, and both HY-80 and CS materials.

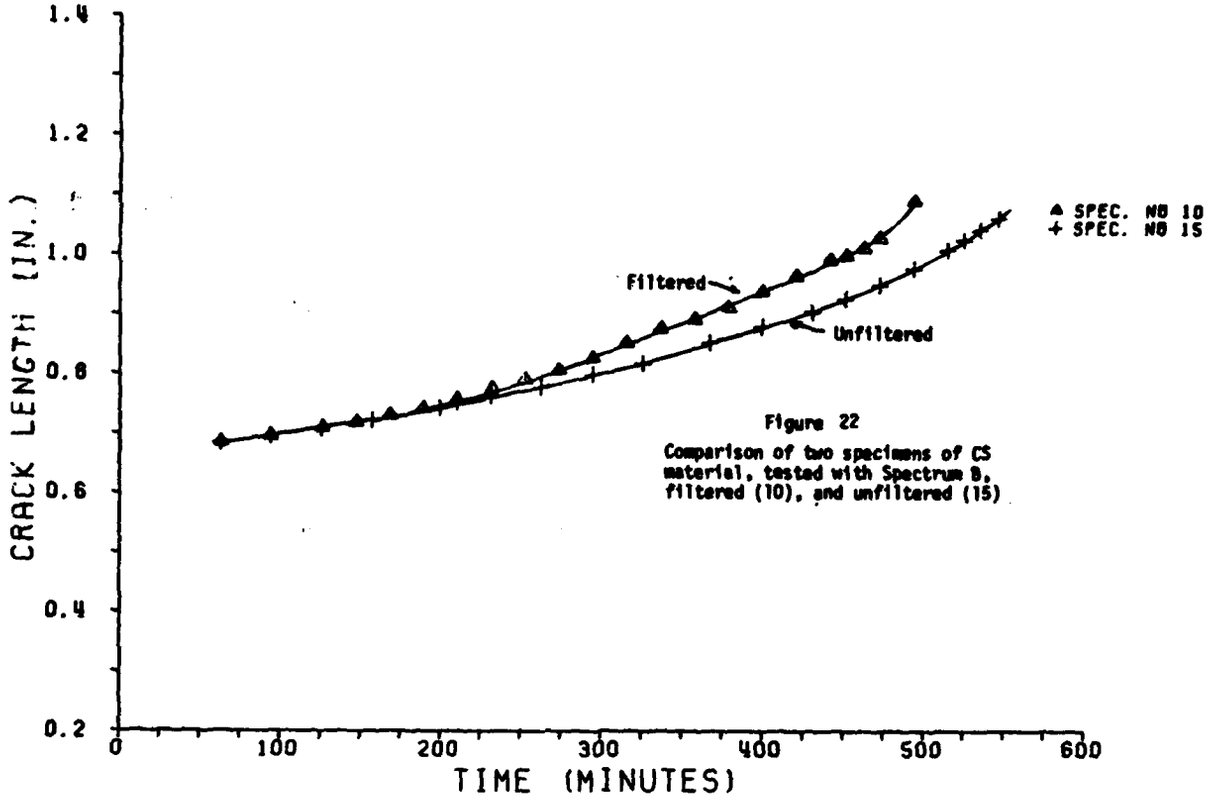

Figure 22

Comparison of two specimens of CS material, tested with Spectrum B, filtered (10), and unfiltered (15)

CRACK LENGTH VS. TIME

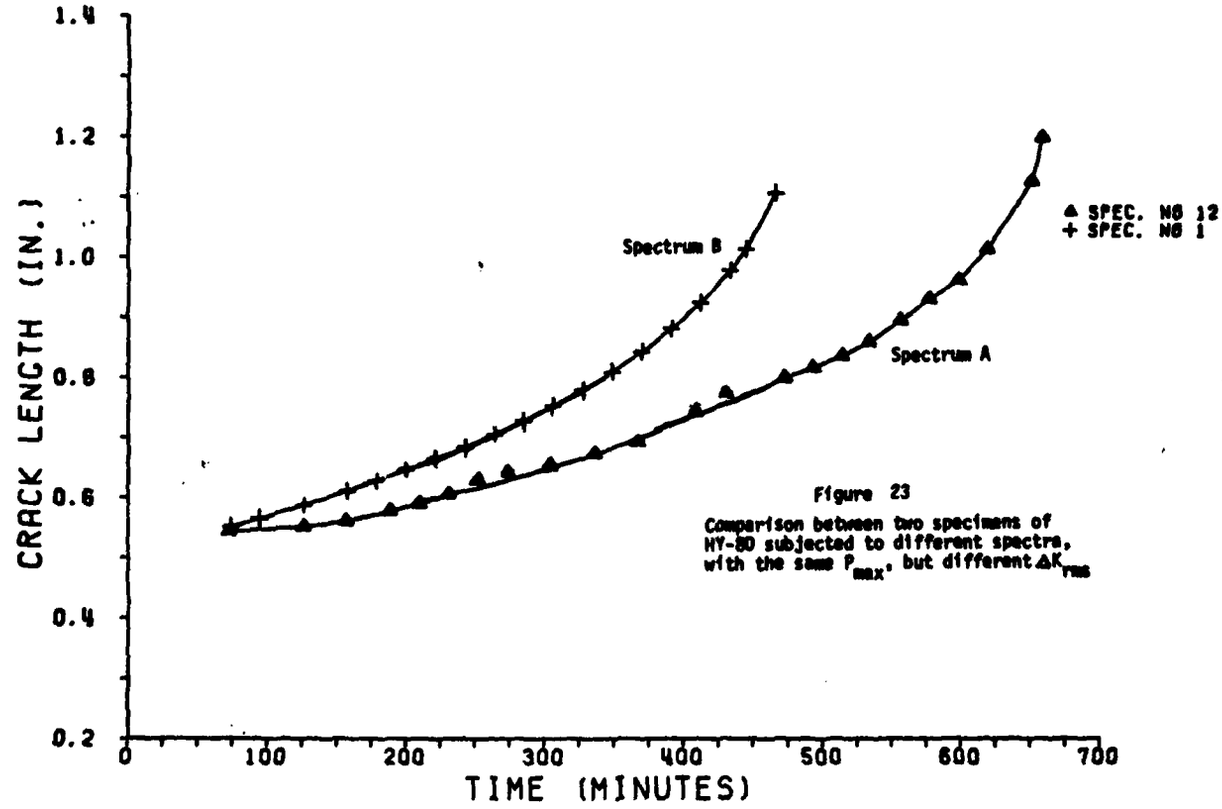

Figure 23

Comparison between two specimens of HY-80 subjected to different spectra, with the same P_{max}, but different ΔK_{rms}

CRACK LENGTH VS. TIME

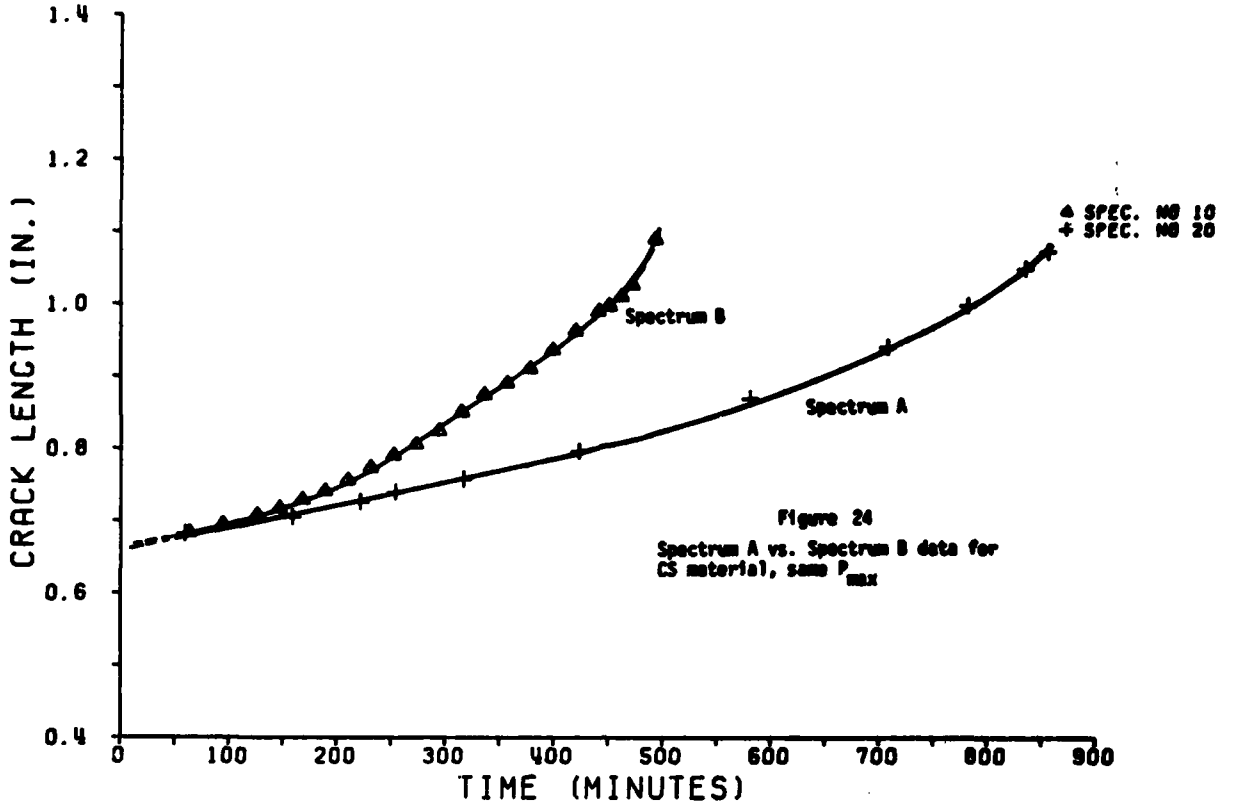

Figure 24
Spectrum A vs. Spectrum B data for CS material, same P_{max}

CRACK LENGTH VS. TIME

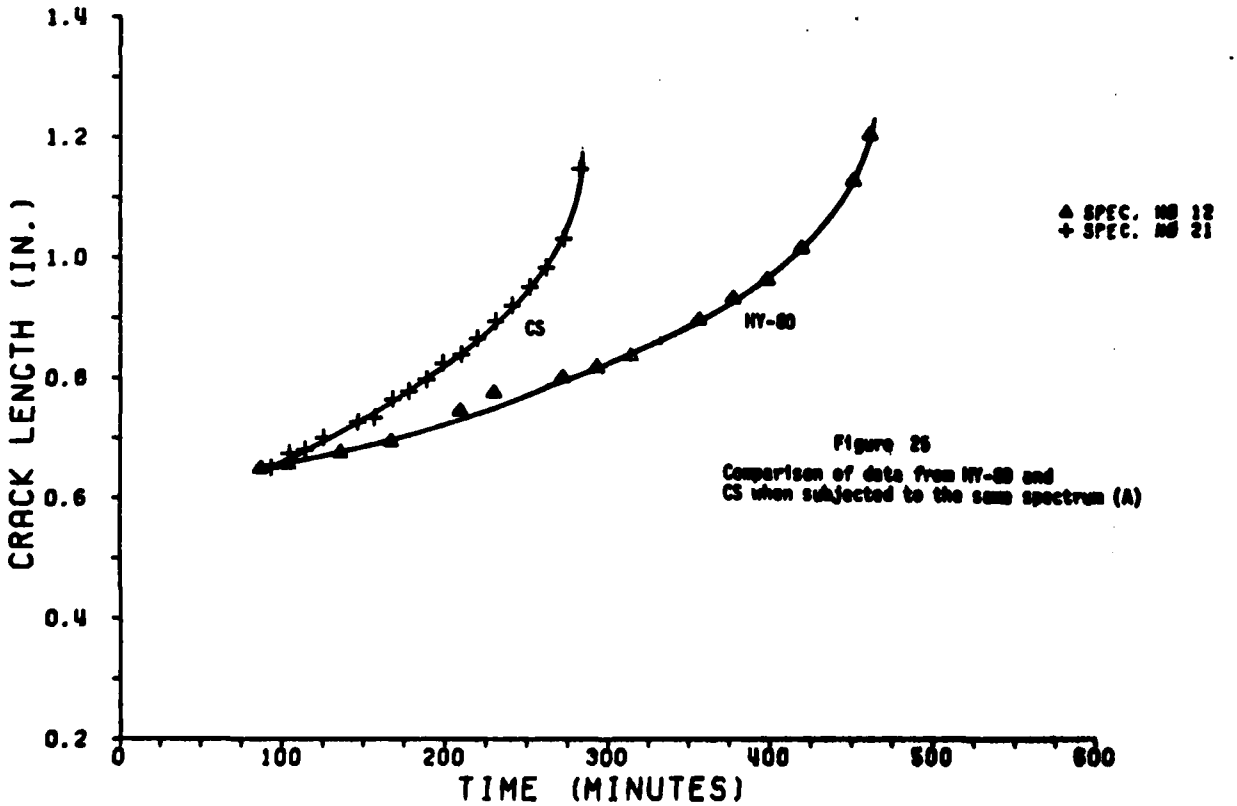

Figure 25
Comparison of data from HY-80 and CS when subjected to the same spectrum (A)

CRACK LENGTH VS. TIME

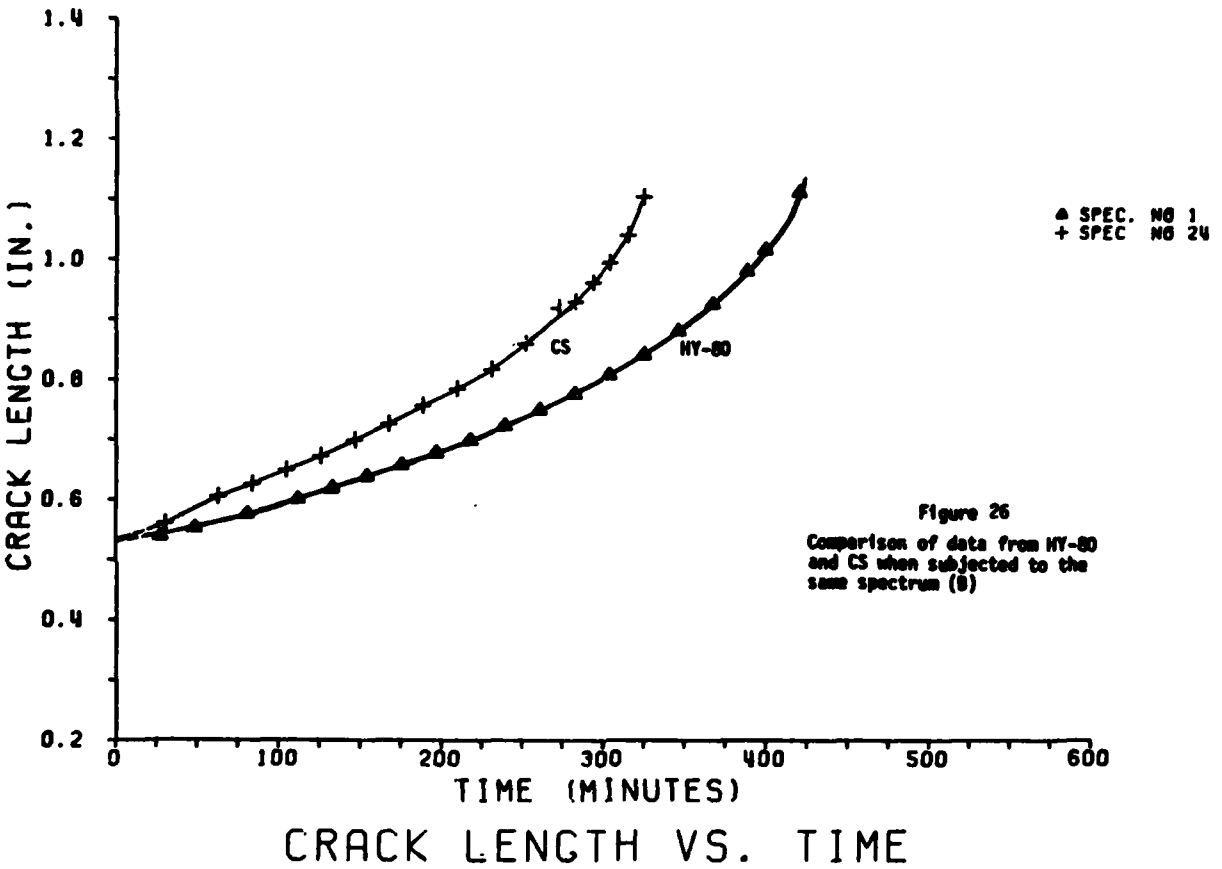

CRACK LENGTH VS. TIME

Figure 26

Comparison of data from HY-80 and CS when subjected to the same spectrum (B)

Presented in Figures 27 and 28 are da/dn versus ΔK_{rms} data for the HY-80 material and the CS material. A linear least-squares fit to the da/dn versus ΔK_{rms} for both materials resulted in the following Paris equation constants:

	HY-80	CS
C	2.64×10^{-9}	1.22×10^{-9}
m	2.37	2.72

4.5 Random Loading- ΔK_{th}

As previously noted, in constant-amplitude testing both the HY-80 and CS materials exhibited threshold stress intensities below which crack propagation did not occur. Similar crack-growth thresholds were not observed for either material when subjected to random loading. The data presented in Figures 27 and 28 do not go below da/dn = 10^{-6} in/cycle or ΔK =10 ksi $\sqrt{in}$. However TES has data as low as ΔK = 7 ksi $\sqrt{in}$ and da/dn = 7×10^{-7} in/cycles. No threshold was noted down to these levels.

4.6 Analytical Results

Crack growth (a versus t) predicted using the Paris equation was faster than crack growth actually observed, demonstrating that crack retardation had occurred. The amount of retardation varied depending upon the material, initial crack length and maximum load. The amount of retardation varied approximately by a factor of 2 to 4. Examples of predictions versus actual experimental results are shown in Figures 29, 30, and 31.

Predicted crack growth depended upon whether a filtered or unfiltered spectrum was used. When the spectra are filtered, faster crack growth by a factor of about 2 is predicted for both spectra as shown in Figures 32 and 33.

Conventional fracture mechanics predicted Spectrum B to have lower crack growth than Spectrum A, when, in fact, it was observed experimentally that Spectrum B produced faster crack growth.

5.0 DISCUSSION OF RESULTS

5.1 Crack Retardation

That crack retardation can occur in structures subjected to load sequences characteristic of the two short-term loadings experienced by the SEA-LAND McLEAN has been demonstrated in this program by Figures 29, 30, and 31. These figures graphically demonstrate the inadequacy of conventional fracture mechanics to predict random loading crack growth. Further confirmation of this is found in the observations that 1) conventional fracture mechanics predicts Spectrum A to cause cracks to grow faster than Spectrum B for a given P_{max} and R value, when, in fact, experimental results show Spectrum B will grow cracks faster, and 2) conventional fracture mechanics predict different crack-growth rates for filtered and unfiltered spectra, when, in fact, there is little difference.

Random Loading
Figure 27c
Figure 27b
Figure 27a

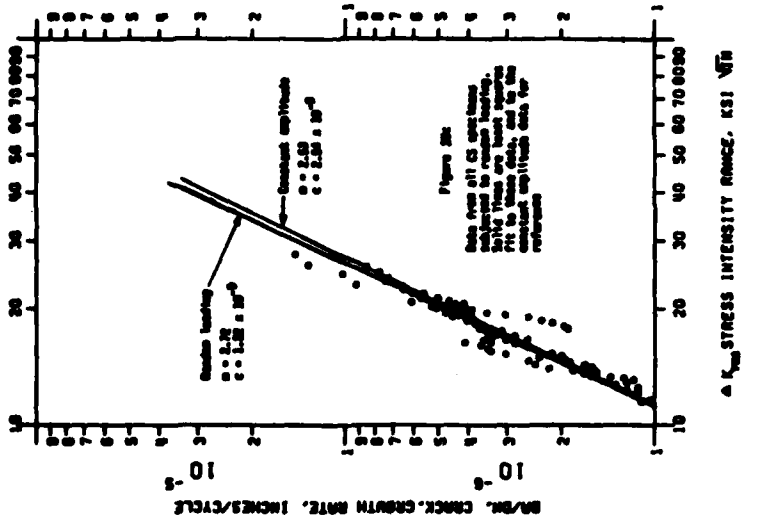

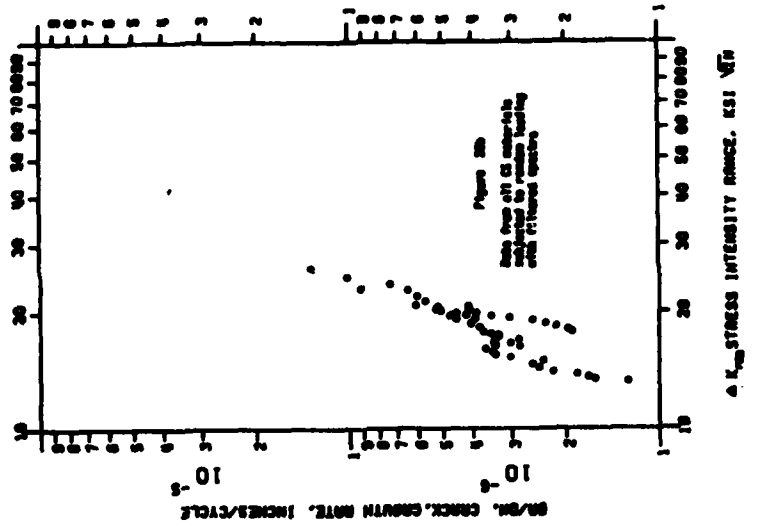

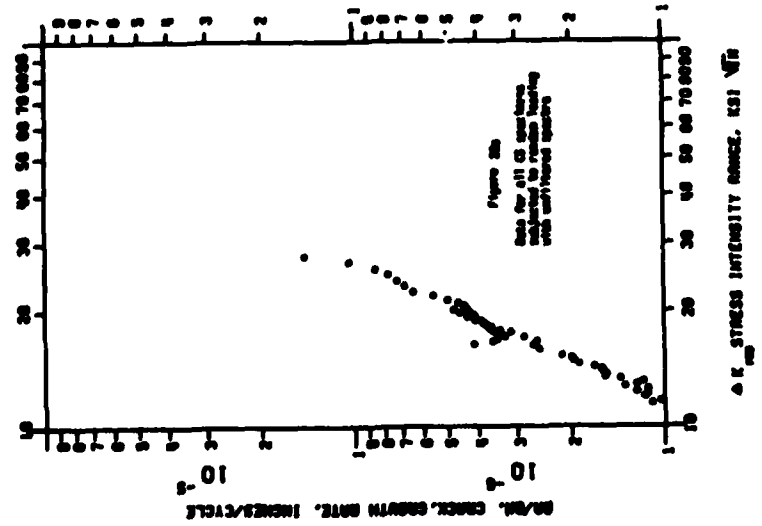

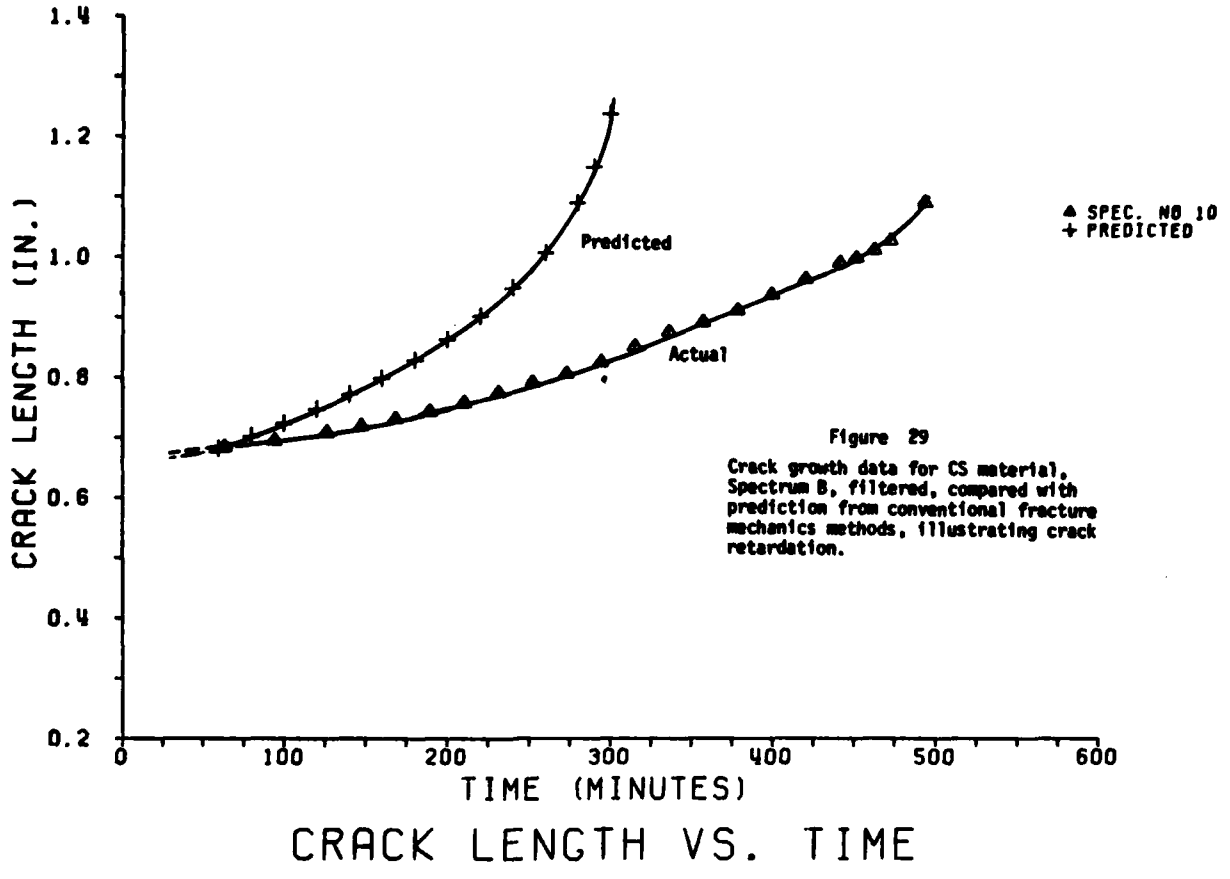

Figure 29

Crack growth data for CS material, Spectrum B, filtered, compared with prediction from conventional fracture mechanics methods, illustrating crack retardation.

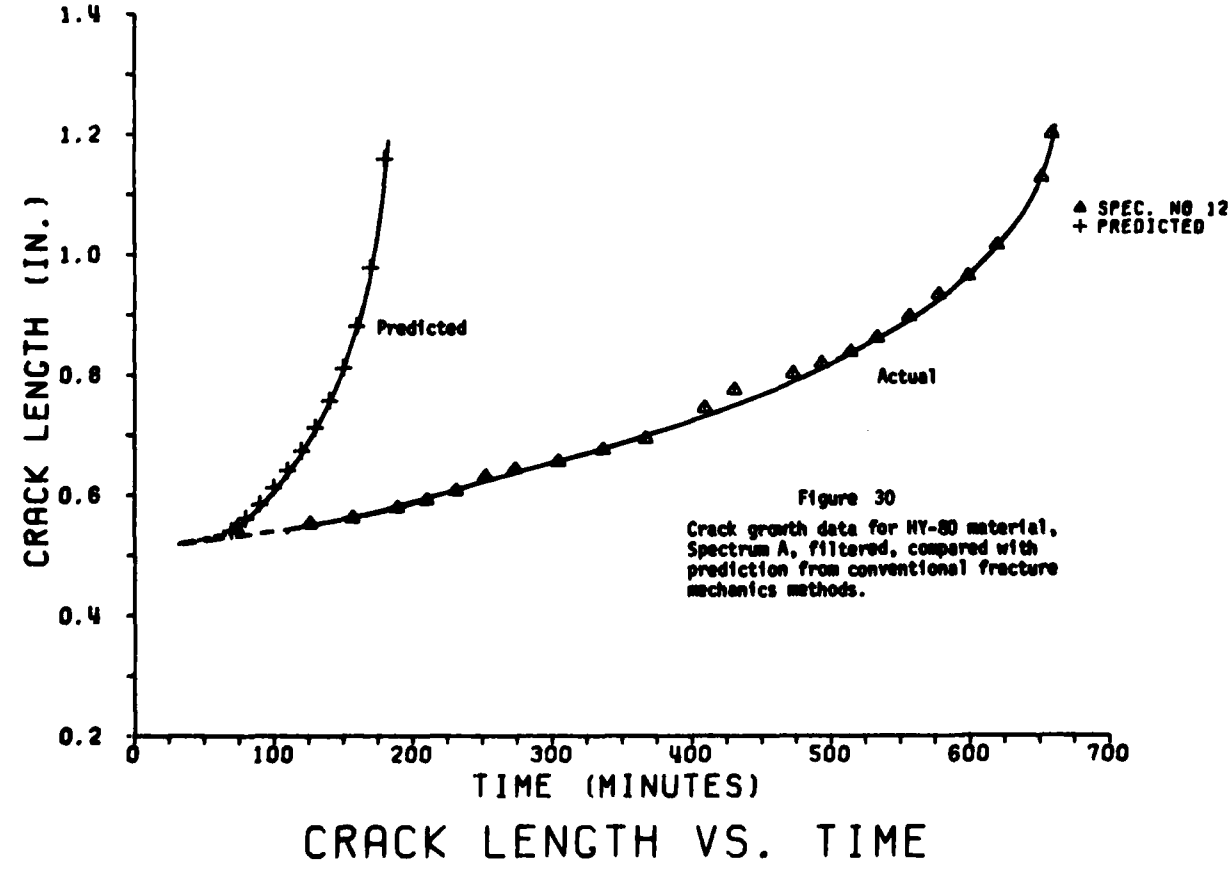

Figure 30

Crack growth data for HY-80 material, Spectrum A, filtered, compared with prediction from conventional fracture mechanics methods.

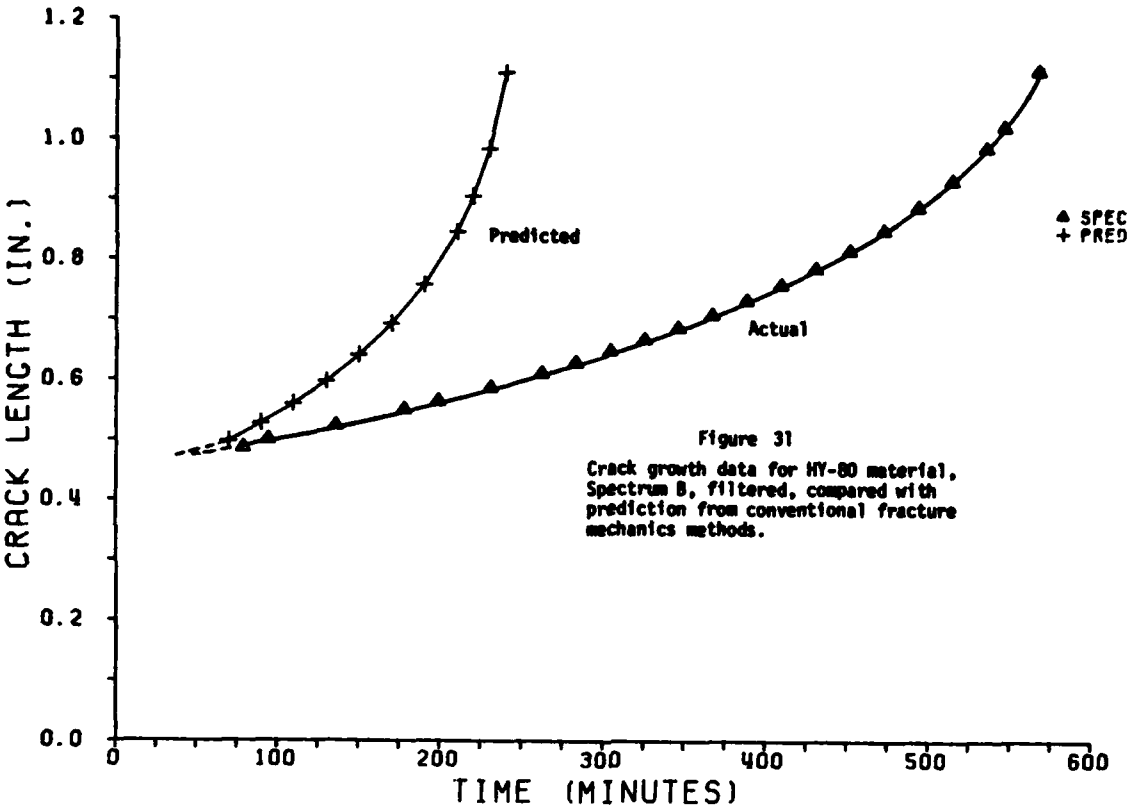

Figure 31

Crack growth data for HY-80 material, Spectrum B, filtered, compared with prediction from conventional fracture mechanics methods.

CRACK LENGTH VS. TIME

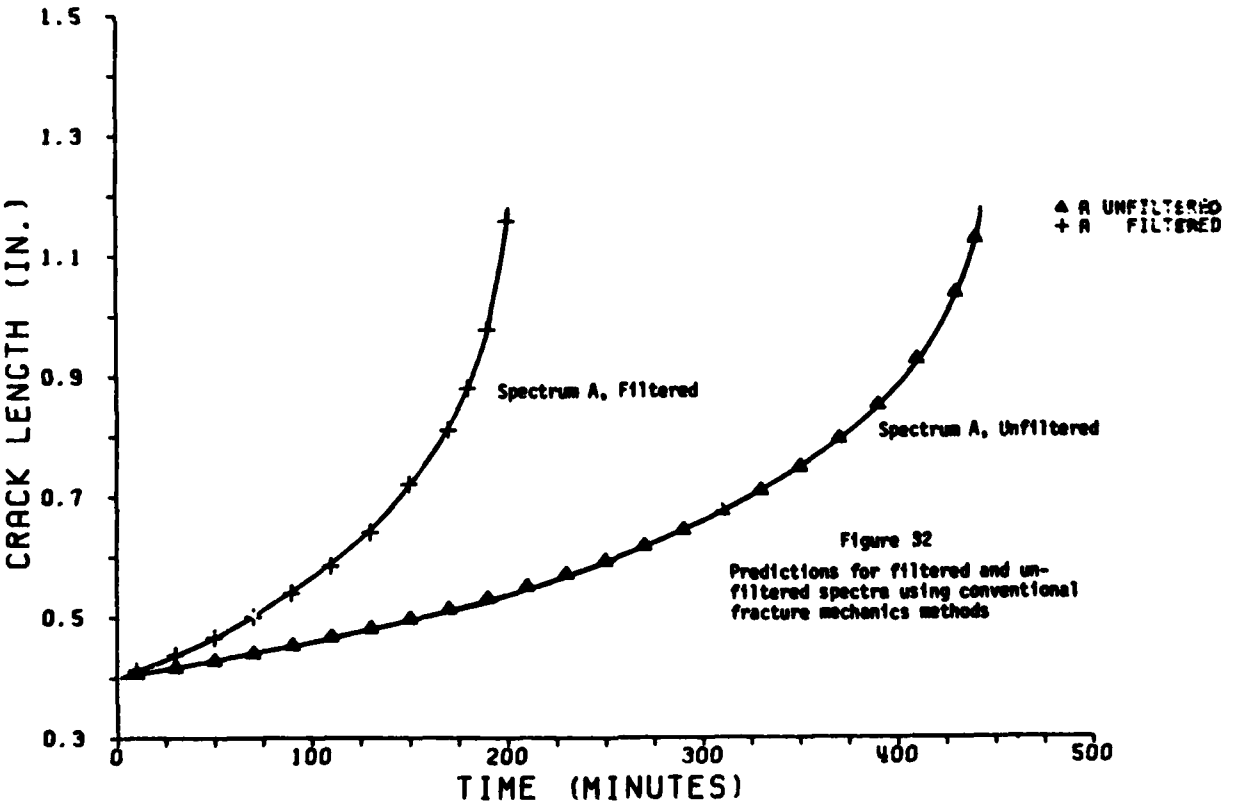

Figure 32

Predictions for filtered and unfiltered spectra using conventional fracture mechanics methods

CRACK LENGTH VS. TIME

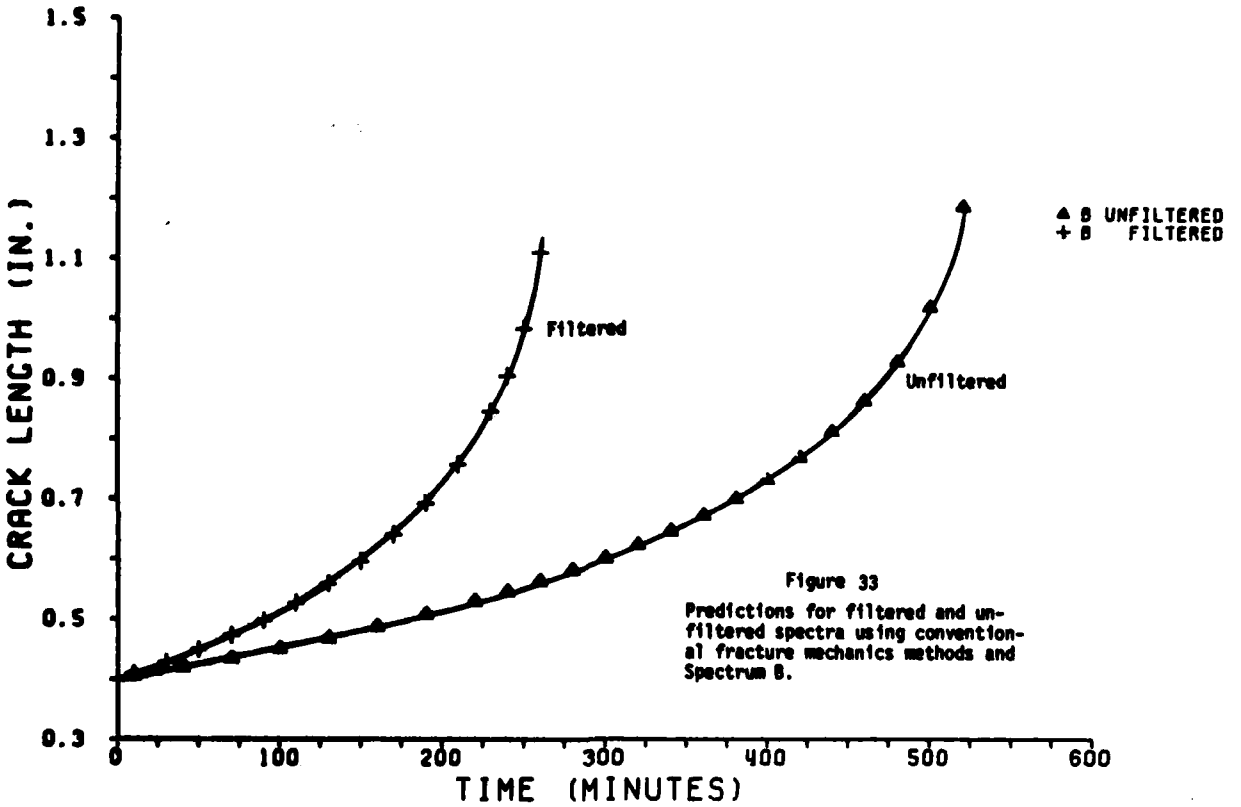

Figure 33

Predictions for filtered and unfiltered spectra using conventional fracture mechanics methods and Spectrum B.

CRACK LENGTH VS. TIME

5.2 Constant-Amplitude Fatigue Crack Propagation

5.2.1 HY-80 Material

A linear least-squares fit to the constant-amplitude data found the constants C and m to be

$$C = 0.177 \times 10^{-8}$$
$$m = 2.54$$

Other investigators (17) have found that for martensitic steels (such as HY-80) as a class, m was 2.25, and C ranged from 0.27 to 0.66×10^{-8}. HY-80 itself was found to be much closer to a value of 0.27×10^{-8} for C. When compared with the data plotted in Figure 13.39 of Reference 17, the experimental results fall within the scatter band, even though the slope and intercept of the least-squares line are slightly different. Thus, the results of this investigation found the HY-80 crack-growth properties to be similar to those reported previously.

5.2.2 CS Material

A linear least-squares fit to the constant-amplitude data for the CS material found the constants C and m to be:

$$C = 0.254 \times 10^{-8}$$
$$m = 2.53$$

No comparable results were available in the literature for this material. However, these numbers indicate a faster crack-growth rate for the CS material than for the HY-80. This is surprising in view of the fact that HY-80 is a martensitic steel, which, as a class, generally has higher crack-growth rates than lower-strength steels such as this CS material. Note that under random loading HY-80 also had a slower crack-growth rate than the CS material.

5.3 Threshold Crack Growth

The HY-80 had a higher threshold (ΔK_{th}) for beginning of crack growth compared to the CS material. This is to be expected since martensitic materials as a class have higher thresholds than lower strength materials. What is surprising is that the threshold in either case is 10 ksi$\sqrt{\text{in}}$ or higher. Many references show that typical thresholds for steels are in the range of 5-6 ksi$\sqrt{\text{in}}$ without much effect due to alloying or strength level (17). An explanation of why the threshold determined in this study is so comparatively high has not been found, although it may be the way in which ΔK_{th} was defined in this study.

The data reported here show no apparent threshold for specimens of either material subjected to random loads. It was intended that the experiment would generate data only in the Stage II crack growth range, and such data is reported here. However, TES does have some crack growth data below da/dn = 10^{-6} in/cycle and ΔK down to 7 ksi $\sqrt{\text{in}}$. In this data, no threshold is apparent.

It is possible that a threshold may exist at some lower value of K. It is more likely that a random-load threshold does not exist since, under random loading, no matter how low one goes in ΔK_{rms} there will always be a few cycles at some ΔK_{max} much greater than ΔK_{rms}, which will be in the range of Stage II crack growth. Therefore, crack extension will continue to occur even though ΔK_{rms} is well below the ΔK_{th} from constant-amplitude tests.

5.4 ΔK_{rms} Model

The data show that, on the average, da/dn is a function of ΔK_{rms} whether the test is for constant or variable amplitude random loading. The variations in C and m between the constant and variable amplitude data are well within the experimental error typically found in crack-growth studies (22, 33). In tests conducted in accordance with E-647, a variability of 2 at a given level of ΔK can be expected just due to experimental and material variations (19).

5.5 Effect of High-Frequency, Low-Amplitude Components of Spectrum

This investigation showed that the high-frequency, low-amplitude components of the spectra had no significant effect on crack growth. This was shown by the fact that filtering to remove the high-frequency component produced similar crack-growth rates as the unfiltered signal as shown in Figure 22, and the fact that specimens tested with unfiltered spectra could be treated as if they had been tested with a filtered spectrum. The slight difference in final crack lengths in Figure 22 is within expected experimental error (22, 23).

Further investigation is necessary to determine if additional filtering could be undertaken to simplify the random loading spectra without affecting crack-growth behavior.

When unfiltered data were plotted as da/dn versus ΔK_{rms}, two factors caused the plotted data to be an order of magnitude removed from the constant amplitude da/dn versus ΔK line. First, the additional small cycles which apparently did not contribute to crack growth increased, thereby decreasing the calculated da/dn. Second, these small cycles reduced the calculated ΔK_{rms}. Thus, when crack length versus time was plotted for the conditions of filtered and unfiltered spectra of the same nominal P_{max} and R value, the curves were nearly the same.

Since ΔK_{rms} was not the same for the two conditions, when the data were plotted as da/dn versus ΔK_{rms}, the filtered and unfiltered data did not coincide. But, when the unfiltered data was treated as if it had been filtered data, the plots of da/dn versus ΔK_{rms} were nearly coincident. Therefore, this showed conclusively that the filtering had no effect on crack growth since the information removed by filtering was not contributing to crack growth.

6.0 REFERENCES

1. Wheeler, O.E., Jnrl. of Basic Engineering, ASME Vol. 94, Series D, No. 1, March 1972, pp. 181-186.

2. Willenborg, J., Engle, R.M., and Wood, H.A., "A Crack-Growth Retardation Model Using an Effective Stress Concept," AFFDRL-TR-74-27, Air Force Flight Dynamics Laboratory, July 1974.

3. Morman, K.N., Jr., and Dubensky, R.G., "Predicting Fatigue Crack Retardation under Single and Intermittent Overloading," Cracks and Fracture, ASTM STP 601, 1976, pp. 245-261.

4. Gray, T.D., and Gallagher, J.P., "Predicting Fatigue Crack Retardation Following a Single Overload Using a Modified Wheeler Model," Mechanics of Crack Growth, ASTM STP 590, 1976, pp. 331-344.

5. Hardrath, H.R., Newman, J.C., Elber, W., Poe, C.C., "Recent Developments in Analysis of Crack Propagation and Fracture of Practical Materials," NASA Technical Memorandum 78766, June 1978.

6. Chazal, E.A., Jr., et.al., "Third Decade of Research under the Ship Structure Committee," SSC-253, 1976.

7. Fain, R.A., "Design and Installation of a Ship Response Instrumentation System Aboard the SL-7 Class Containership S.Sea-Land McLean," SSC 238, 1974.

8. Boentgen, R.R., Fain, R.A., Wheaton, J.W., "First Season Results From Ship Response Instrumentation Aboard the SL-7 Class Containership S.S. Sea-Land McLean in North Atlantic Service," SSC 264, 1976.

9. Wheaton, J.W., Boentgen, R.R., "Second Season Results From Ship Response Instrumentation Aboard the SL-7 Class Containership S.S. Sea-Land McLean in North Atlantic Service," 1976, AD-A034162.

10. Boentgen, R.R., "Third Season Results From Ship Response Instrumentation Aboard the SL-7 Class Containership S.S. Sea-Land McLean in North Atlantic Service," 1976, AD-A034175.

11. Naval Ship Engineering Center, Department of the Navy, Washington, D.C., "Ship Hull Characteristics Program--SHCP User's Manual, January, 1979.

12. Vossers, G., Swann, W.A., and Rijken, H., "Vertical and Lateral Bending Moment Measurements on Series 60 Models," International Shipbuilding Progress, Vol. 8, No. 83, July 1961.

13. Jasper, N., "Temperature-Induced Stresses in Beams and Ships," ASME Journal, August 1956, p. 485.

14. Crutcher, H.K., and Davis, O.M., "Marine Climatic Atlas of the World," U.S. Navy, NAVIAR 50-K-54, March 1, 1969.

15. Lewis, E.V., Hoffman, D., MacLean, W.M., VanHooff, R., and Zubaly, R.B., "Load Criteria for Ship Structural Design," SSC-240, 1973.

16. Stiasen, S.G., and Chen, H.H., "Application of Probabilistic Design Methods to Wave Loads Prediction for Ship Structures Analysis," American Bureau of Shipping, November 1979.

17. Hertzberg, R.W., Deformation and Fracture Mechanics of Engineering Materials, John Wiley and Sons, 1976.

18. Barsom, J.M., Novak, S.R., "Subcritical Crack Growth and Fracture of Bridge Steels," National Cooperative Highway Research Program Report 181, Transportation Research Board, Washington, D.C., 1977.

19. Saxena, A., Hudak, S.J., Jr., "Review and Extension of Compliance Information for Common Crack Growth Specimens," International Journal of Fracture, Vol. 14, No. 5, pp. 453-468, October 1978.

20. Abelkis, P.R., editor, "Service Fatigue Loads Monitoring, Simulation, and Analysis," ASTM STP 671, 1974.

21. Fuchs, H.O., Stephens, R.I., Metal Fatigue in Engineering, John Wiley and Sons, 1980, pp. 196-203.

22. Virkler, D.A., Hillberry, B.M., Goel, P.K., "The Statistical Nature of Fatigue Crack Propagation," Trans. ASME Ser. H., Vol. 101, p. 149, April 1979.

23. "Tentative Test Method for Constant-Load-Amplitude Fatigue Crack Growth Rates Above 10^{-8} m/cycle." ASTM Designation E647-78T, Annual Book of ASTM Standards for 1978, Part 10, pp. 662-679.

☆U.S. GOVERNMENT PRINTING OFFICE: 1984-421-428/3551

Committee on Marine Structures
Marine Board
National Academy of Sciences - National Research Council

The Committee on Marine Structures (Formerly Ship Research Committee) has technical cognizance of the Interagency Ship Structure Committee's research program. For this project, SR-1266, they prepared the project prospectus provided the technical guidance, and reviewed the project report with the investigators.

Mr. A. D. Haff, Chairman, Annapolis, MD
Prof. A. H.-S. Ang, University of Illinois, Champaign, IL
Dr. K. A. Blenkarn, Amoco Production Company, Tulsa, OK
Mrs. Margaret Ochi, Gainesville, PA
Mr. D. Price, National Oceanic and Atmospheric Administration, Rockville, MD
Mr. D. A. Sarno, ARMCO Inc., Middletown, OH
Mr. J. E. Steele, Naval Architect, Quakertown, PA
Mr. R. W. Rumke, Executive Secretary, Committee on Marine Structures

MATERIALS ADVISORY GROUP

The Materials Advisory Group prepared the project prospectus and evaluated the proposals for this project.

Mr. D. A. Sarno, Chairman, ARMCO Inc., Middletown, OH
Dr. R. Bicicchi, Sun Tech. Inc., Chester, PA
Dr. C. M. Fortunko, National Bureau of Standards, Boulder, CO
Prof. G. T. Hahn, Vanderbilt University, Nashville, TN
Dr. N. Zettlemoyer, Exxon Production Research Company, Houston, TX

FATIGUE PROGRAM ADVISORY COMMITTEE

The Fatique Program Advisory Committee provided the liaison technical guidance, and reviewed the project with the investigator.

Mr. P. W. Marshall, Shell Oil Company, Houston, TX
Dr. R. D. Glasfeld, General Dynamics, Quincy, MA
Prof. P. H. Wirsching, University of Arizona, Tucson, AZ

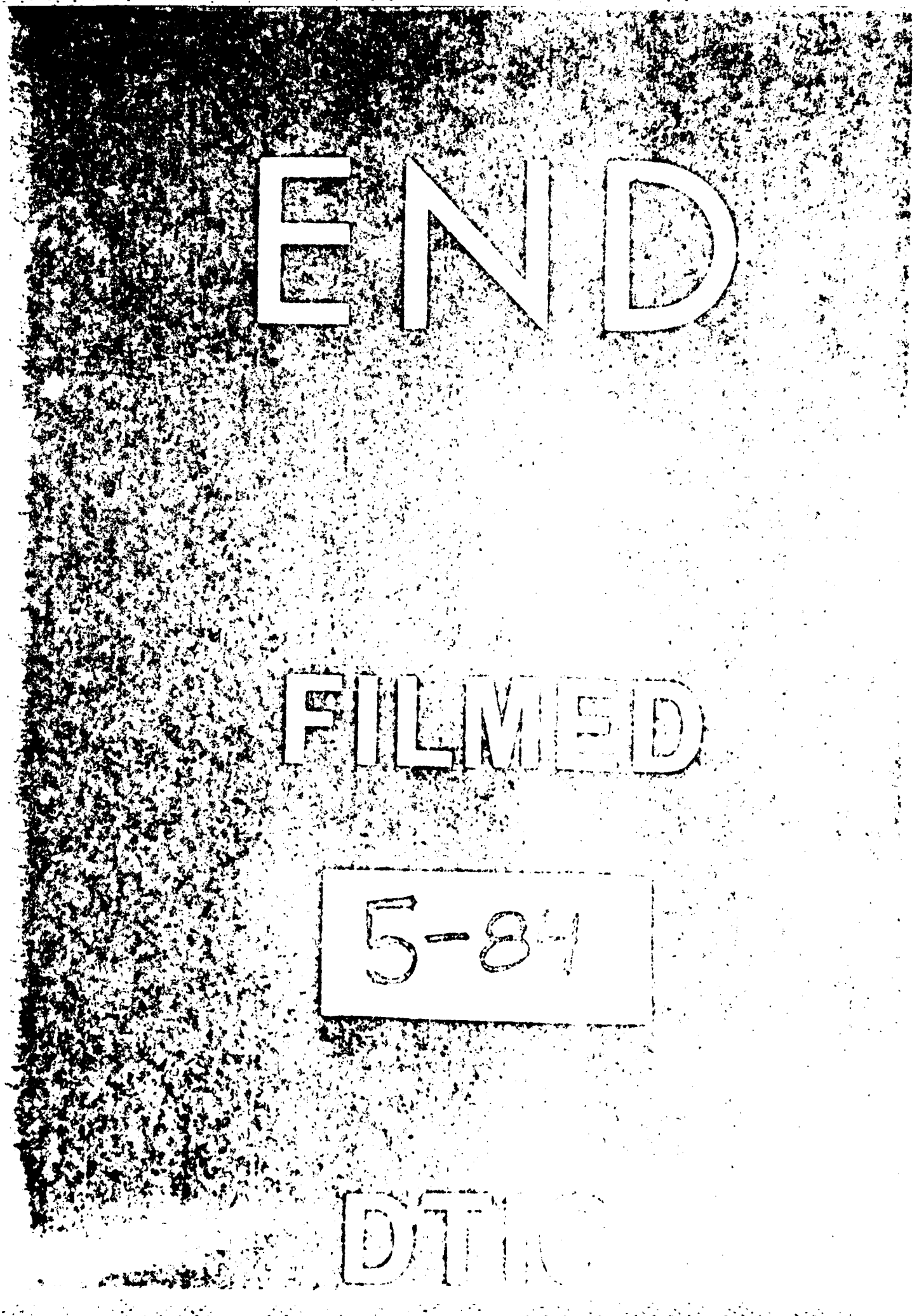
END
FILMED
5-84
DTIC